Correlation of Mathematical Model with AFRL RC-19 Aerothermoelastic Experiment Including an Impinging Shock

AIAA AVIATION Forum 2025

Luisa Piccolo Serafim and Earl Dowell – Duke University

Kirk Brouwer – AFRL, Wright-Patterson AFB

July 22, 2025 | Las Vegas, NV

Duke

Motivation for this Work

- To provide the highest possible fidelity in the computational model at an affordable cost; orders of magnitude reduction in cost compared to traditional CFD/CSD methods
- To explore a wide range of relevant parameters including M_∞, Re, static pressure differential, thermal stresses and structural boundary conditions, both out of plane and in plane.
- **To correlate computational results with experimental results and assess the sensitivity of these results to uncertainties in key parameters**

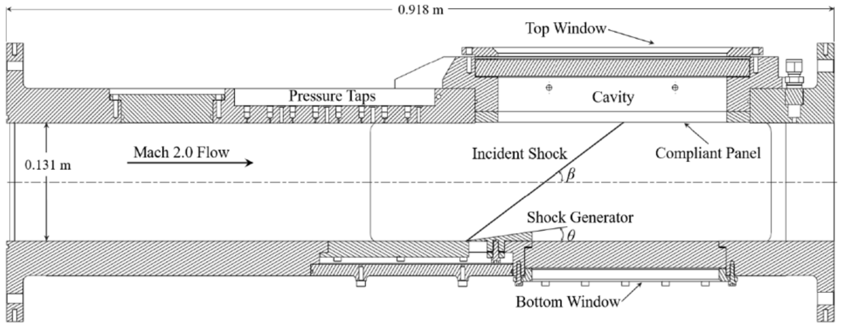

Brouwer et al. AIAAJ (2021)

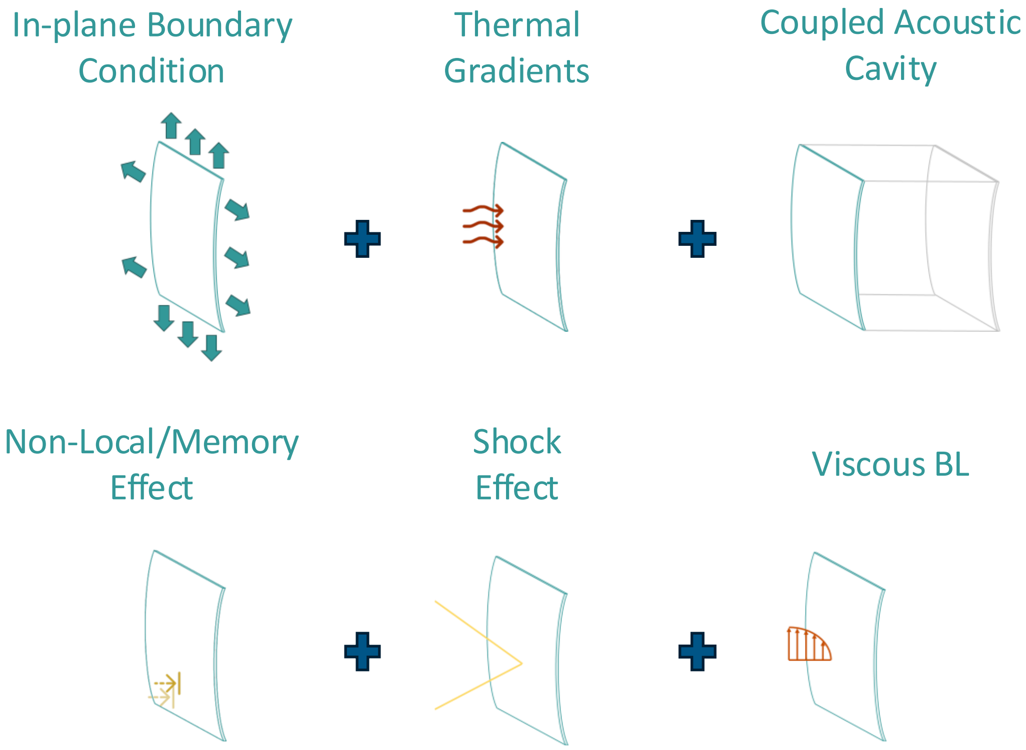

Mathematical/Computational Modeling

Nonlinear Aeroelastic Solver

Set Boundary Conditions

- p_C fixed
- ΔT fixed
- ICs
- Flow parameters

Compute Structural Matrices

- Geometrical dimensions
- β_{BC} varying per run

Compute Aerodynamic Matrices

- Numerical Methods (ROM): Dynamically Linearized Time-domain Approach

Solve ODE in terms of the generalized coord.

$$\underbrace{M_{mn}\ddot{q}_n(t) + C_{mn}\dot{q}_n(t) + G_{mn}^{(2)}q_n(t)}_{\text{Linear plate model}} + \underbrace{D_{mnrp}^{(2)}q_n(t)q_r(t)q_p(t)}_{\text{NL structural stiffness}} + \underbrace{Q_m^{Aero}}_{\text{Aero}} + \underbrace{Q_m^{static}}_{\text{Static pressure differential}} = 0$$

Duke

ROM to include unsteady aerodynamics into the aeroelastic solution

Step change in the CFD domain for each ψ_{mn} …

… in the panel deformation:

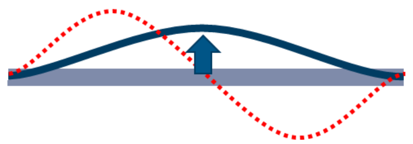

1st set of CFD runs

… in the velocity of the panel deformation:

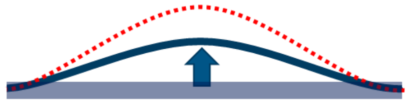

2nd set of CFD runs

… to obtain a pressure field (output) from a known deformation (input)

$$Q_{mn}^{CFD}(t) = \iint \frac{\boxed{\Delta p_m(x,y,t)}}{\rho_\infty U_\infty^2} \psi_n(x,y)\,dx\,dy$$

Work the other way around to obtain the A_{mn}, B_{mn}, and $E_{mn}(t)$ using the input/output relationship

$$Q_{mn}^{CFD}(t) = q_m(t) A_{mn} + \dot{q}_m(t) B_{mn} + \int_0^t q_m(\tau) E_{mn}(t-\tau)\,d\tau$$

Once A_{mn}, B_{mn}, and $E_{mn}(t)$ are obtained, we can reconstruct the Generalized Aerodynamic Force inside the Aeroelastic Solver for any arbitrary panel deformation ($q_m(t)$, $\dot{q}_m(t)$)

$$\boxed{Q_{mn}(t) = q_m(t) A_{mn} + \dot{q}_m(t) B_{mn} + \int_0^t q_m(\tau) E_{mn}(t-\tau)\,d\tau}$$

Experimental Study Case: AFRL/SD RC-19 Wind Tunnel Section

Additional Considerations: In-plane boundary condition

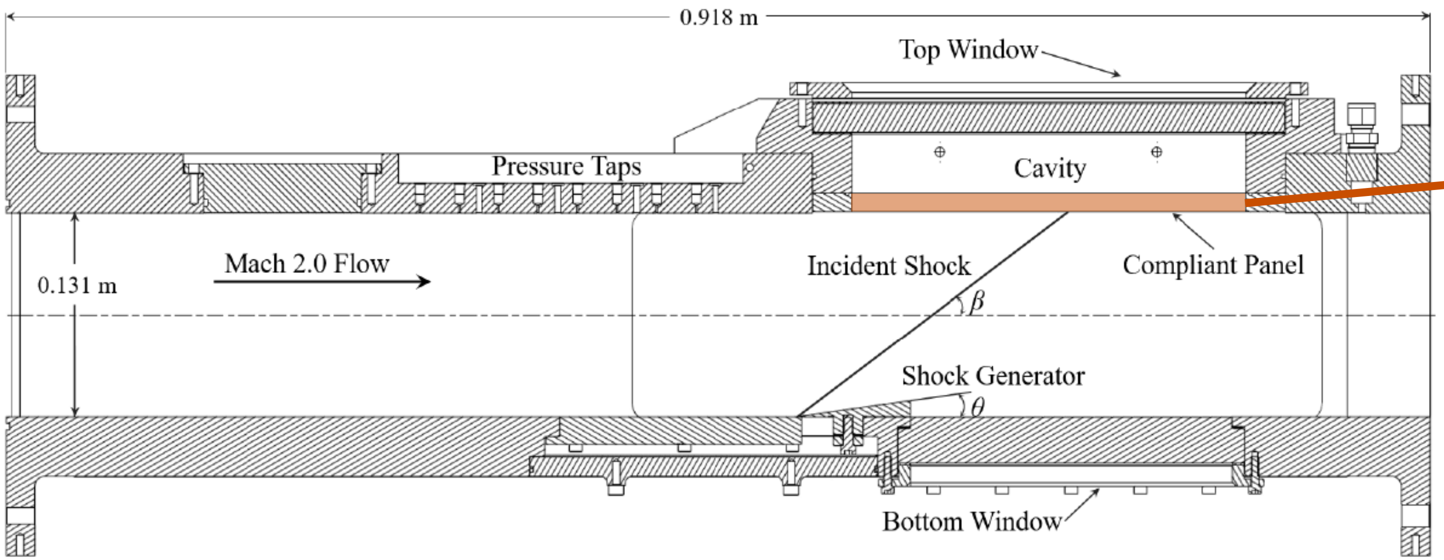

Brouwer et al. AIAAJ (2021)

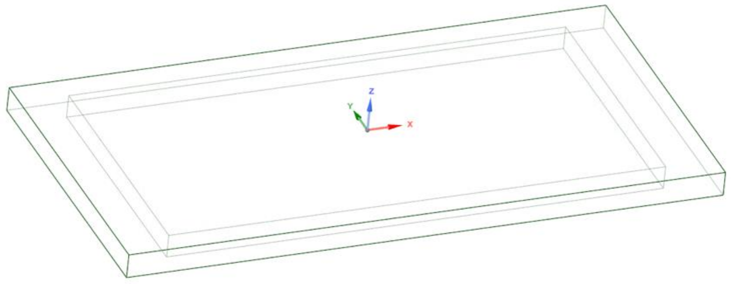

Nonlinear structural behavior

In-plane boundary stiffness

"allowing the panel to deform at the edges as a reaction to the fixed support"

In-plane boundary stiffness

Nondimensional in-plane boundary stiffness

$$\beta_{BC} \equiv \frac{K_{BC}a}{Eh}$$

Panel length

Panel thickness

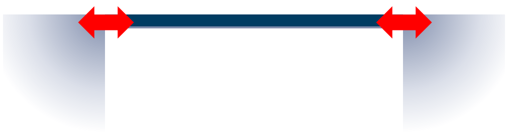

$\beta_{BC} \approx 0$: Free edge displacement

$\beta_{BC} \gg 0$: No edge displacement

Duke

Experimental Study Case: AFRL/SD RC-19 Wind Tunnel Section

Additional Considerations: In-plane boundary condition

Results are presented as a function of the β_{BC}, which is a **structural** parameter

For example:

Mean and STD of the panel deformation at ¾ of the panel length using Linear Piston Theory as the aerodynamic model

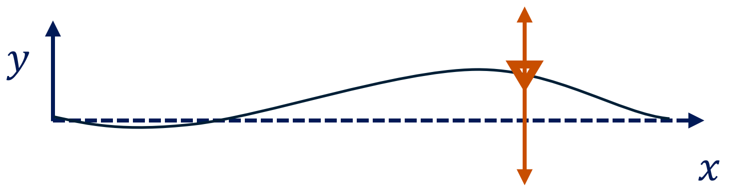

Mean & SDT deformation

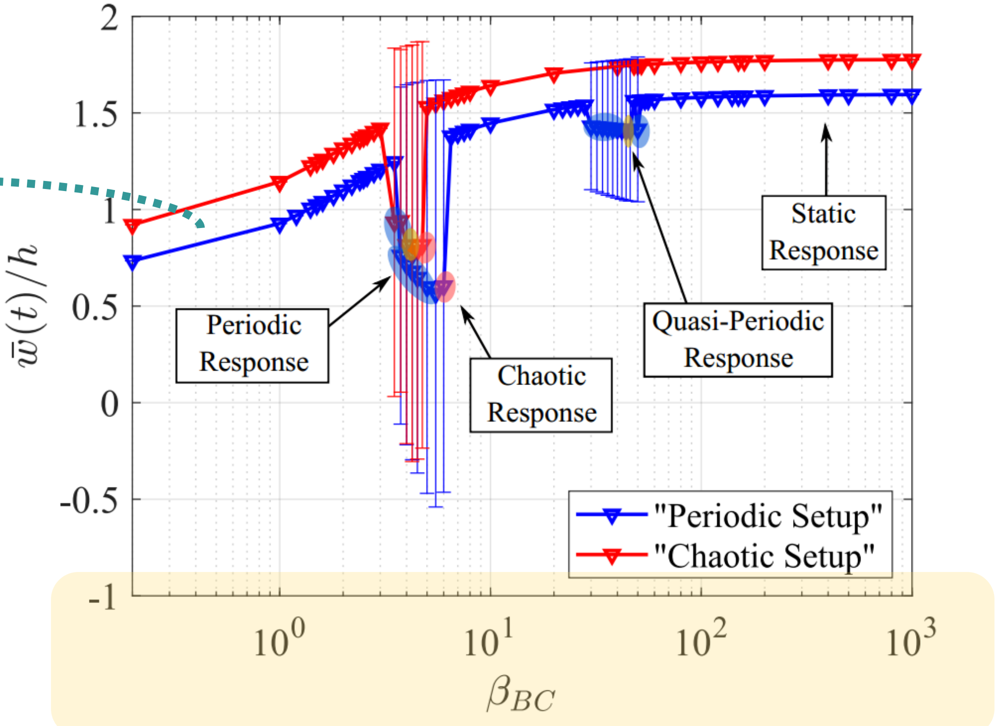

Piccolo Serafim et al. JFS (2023)

DLTA with a Shock Impingement

$\theta = 4^{\circ}$ wedge shock configuration

Aerodynamic Model: Euler (unsteady)/DLTA

(Dynamically Linearized Time-Domain Approach)

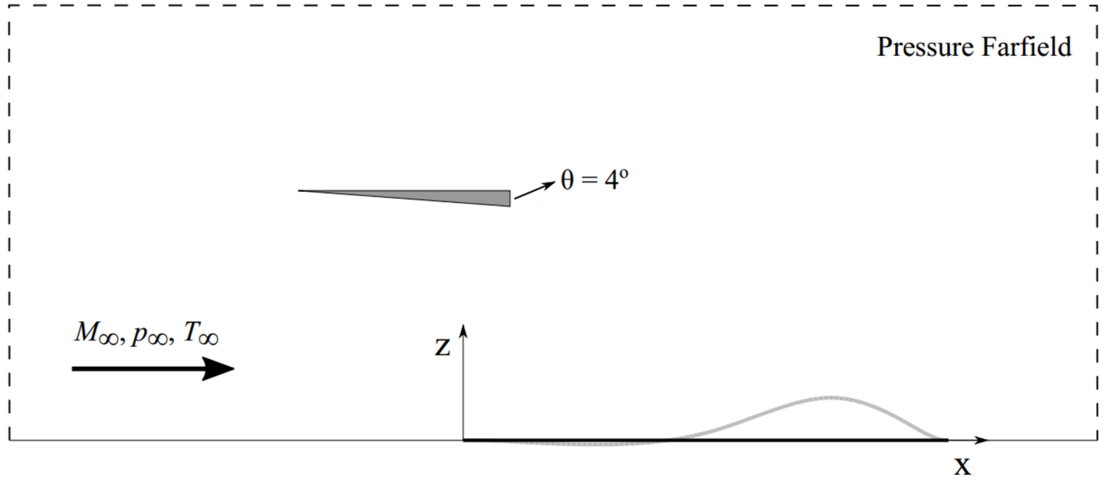

Aerodynamic Model: RANS (unsteady)/DLTA

(Dynamically Linearized Time-Domain Approach)

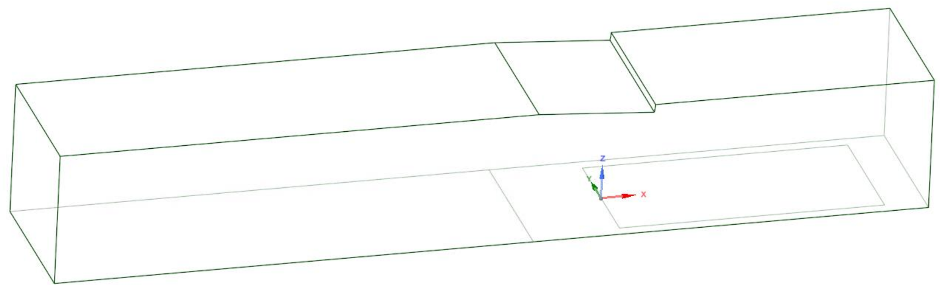

In-Plane boundary stiffness sensitivity

$M_{\infty} = 2.0$

ΔT between panel and frame

Δp between fluid and acoustic cavity

Duke

DLTA with a Shock Impingement

$\theta = 4^{\circ}$ wedge shock configuration

Aerodynamic Model: Euler (unsteady)/DLTA

(Dynamically Linearized Time-Domain Approach)

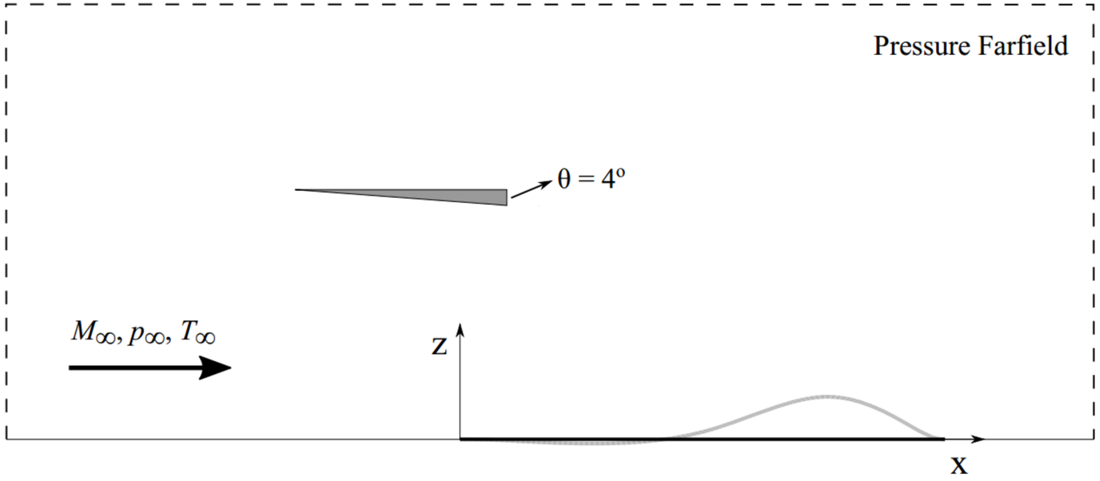

Aerodynamic Model: RANS (unsteady)/DLTA

(Dynamically Linearized Time-Domain Approach)

In-Plane boundary stiffness sensitivity

$M_{\infty} = 2.0$

ΔT between panel and frame

Δp between fluid and acoustic cavity

Duke

DLTA with an Inviscid Shock Impingement

$\theta = 4^{\circ}$ wedge shock configuration

Wind Tunnel Setting

p_c (kPa)	ΔT (K)
68.9	13.3

Mean & SDT deformation
(at ¾ of the panel length)

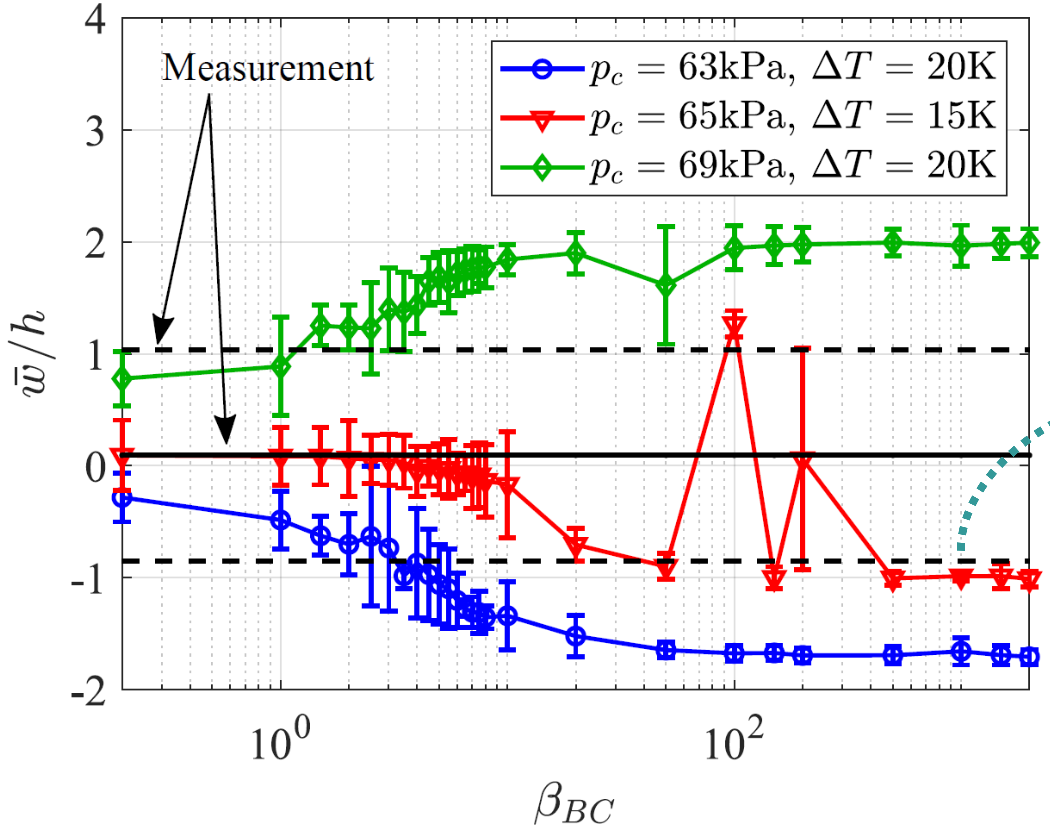

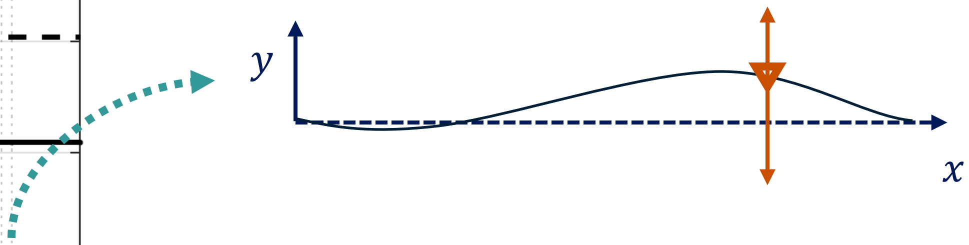

Duke

DLTA with an Inviscid Shock Impingement

$\theta = 4^{\circ}$ wedge shock configuration

Wind Tunnel Setting	
p_c (kPa)	ΔT (K)
68.9	13.3

Mean & SDT deformation

(at ¾ of the panel length)

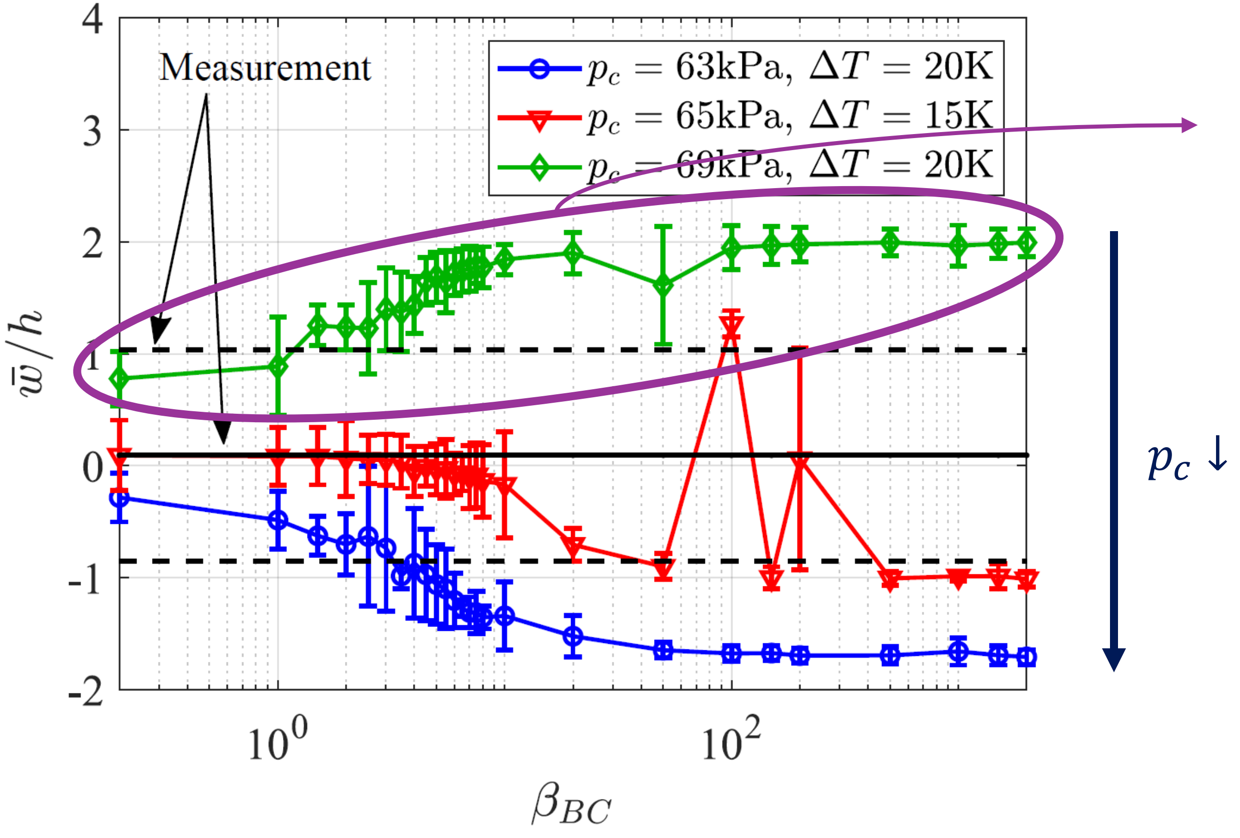

Similar to the wind tunnel setting

Duke

DLTA with an Inviscid Shock Impingement

$\theta = 4^{\circ}$ wedge shock configuration

Mean & SDT deformation
(at ¾ of the panel length)

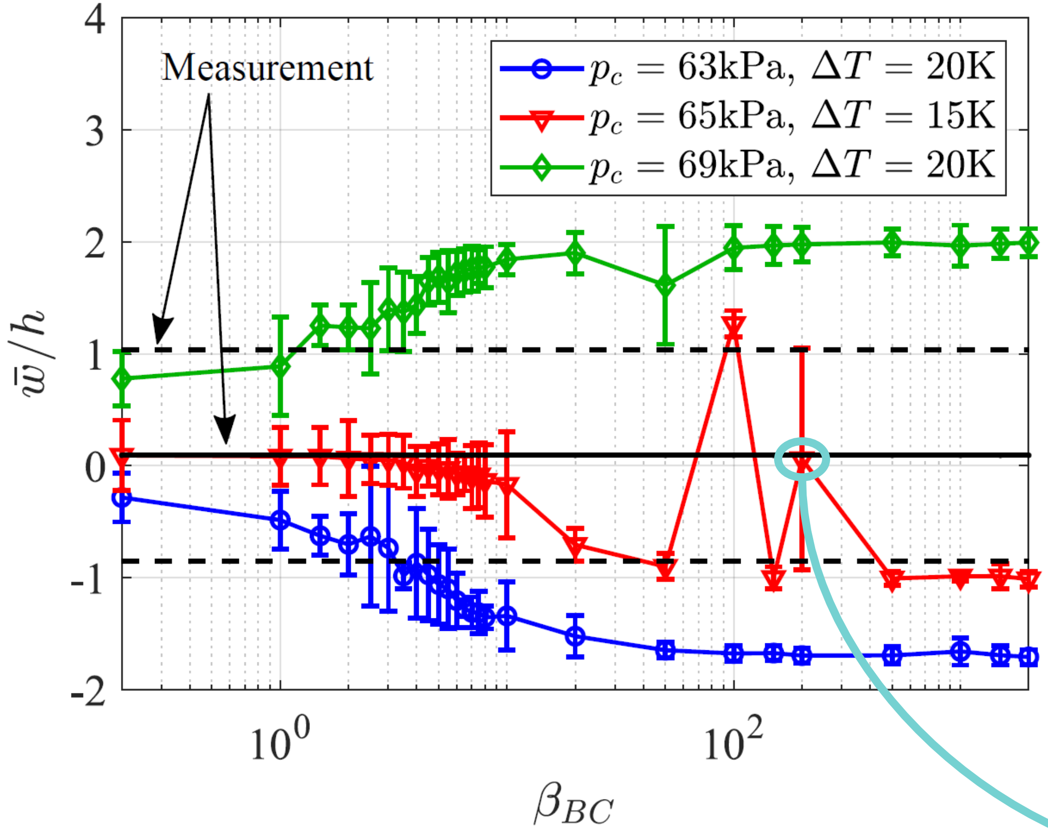

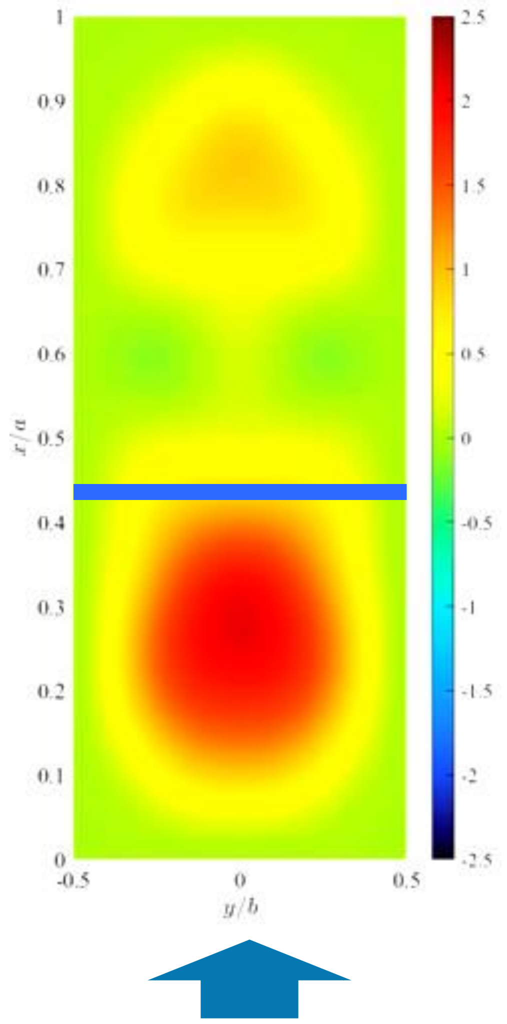

Flow Field

Wind Tunnel Setting

p_c (kPa)	ΔT (K)
68.9	13.3

Duke

DLTA with an Inviscid Shock Impingement

Deformation in time
(at ¾ of the panel length)

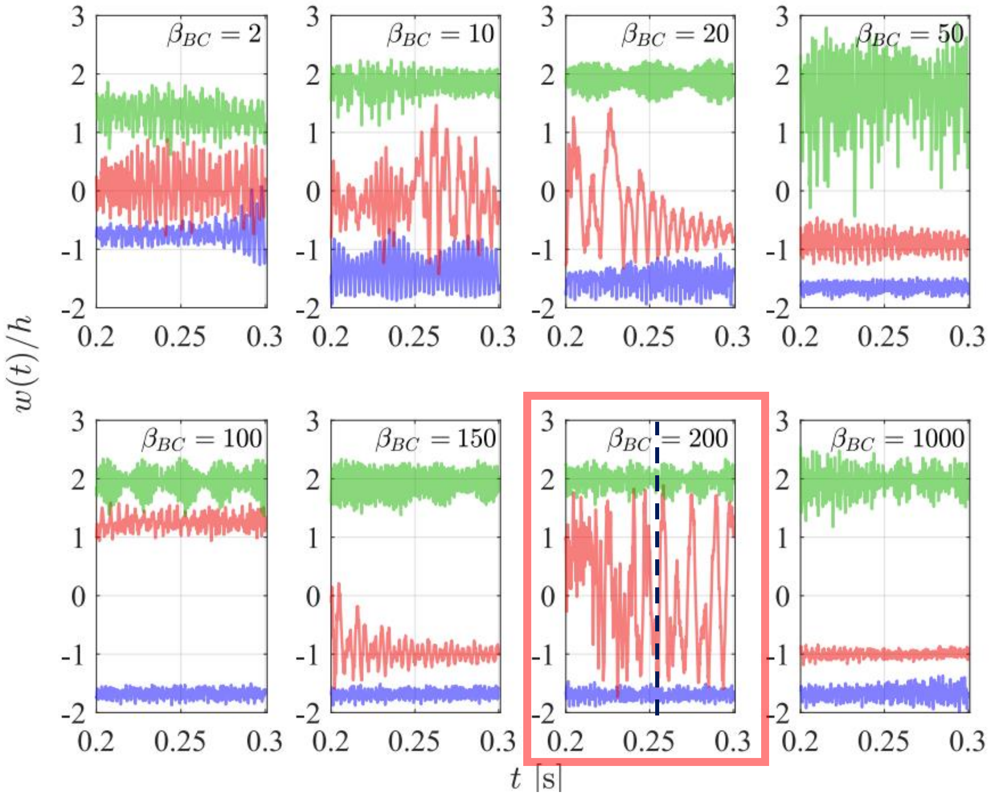

Mean deformation

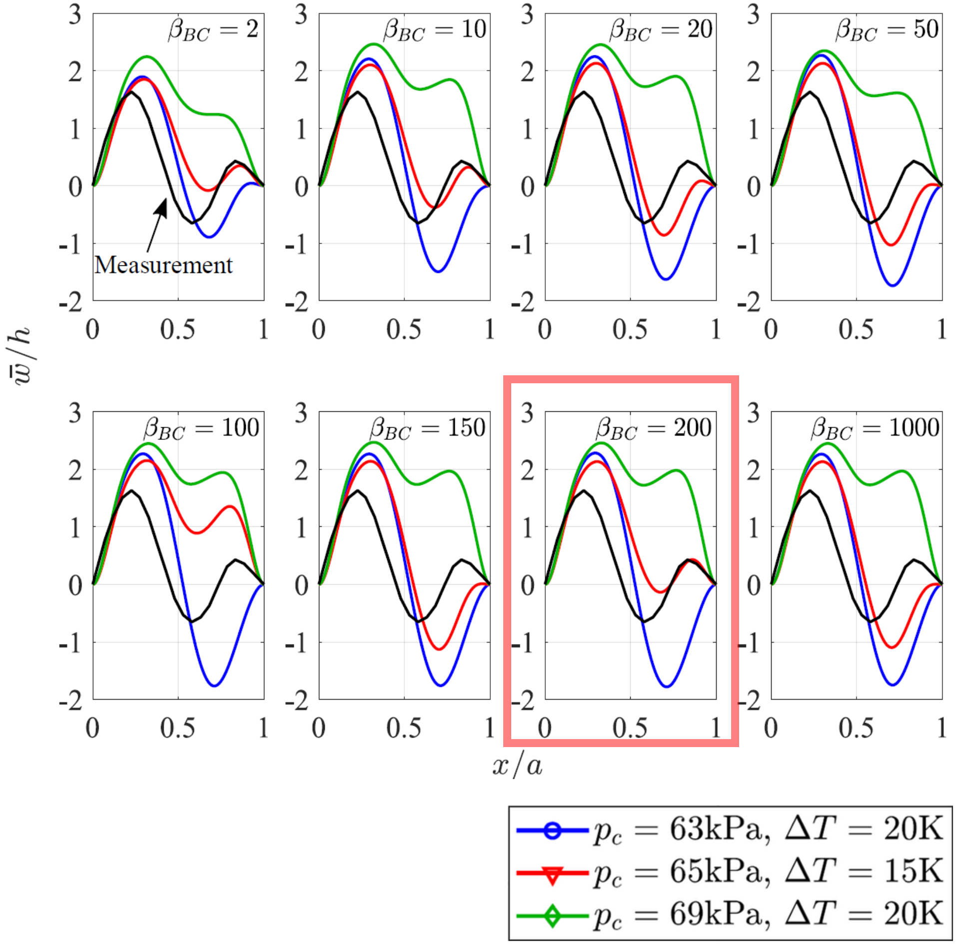

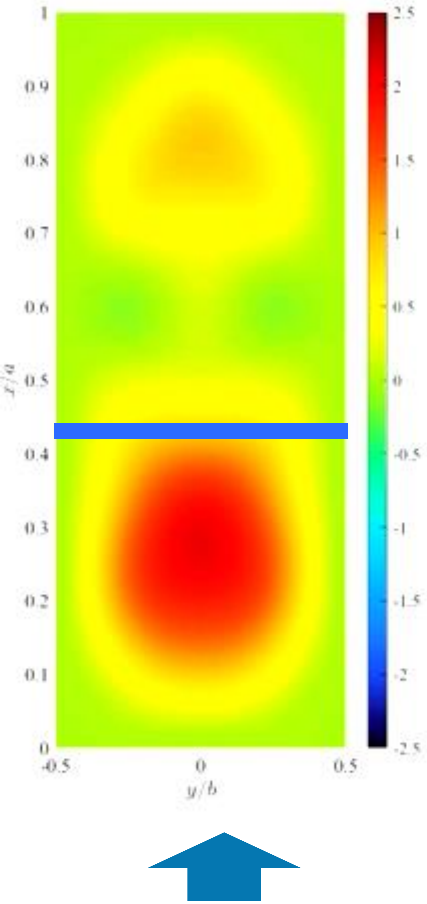

Flow Field

Duke

DLTA with a Shock Impingement

$\theta = 4^{\circ}$ wedge shock configuration

Aerodynamic Model: Euler (unsteady)/DLTA

(Dynamically Linearized Time-Domain Approach)

Aerodynamic Model: RANS (unsteady)/DLTA

(Dynamically Linearized Time-Domain Approach)

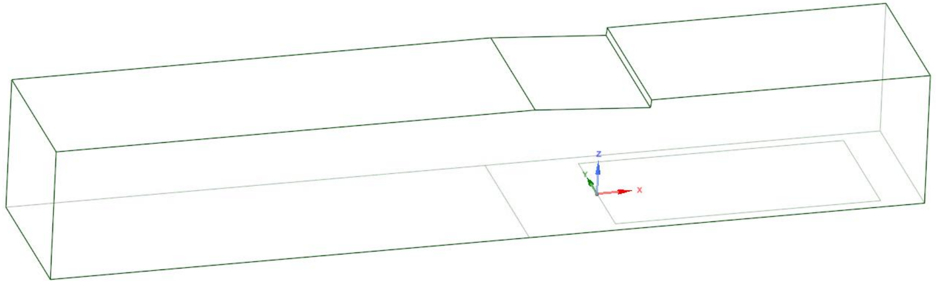

In-Plane boundary stiffness sensitivity

$M_\infty = 2.0$

ΔT between panel and frame

Δp between fluid and acoustic cavity

Duke

DLTA with a Shock Impingement

$\theta = 4^{\circ}$ wedge shock configuration: CFD setup

SST $k - \omega$
$y^{+} = 5$ and 1
$\delta_{LE} \approx 8$mm (Wind Tunnel: $\delta_{LE} \approx 8.6$mm)
$\delta_{LE}/a \approx 0.03$ (Wind Tunnel: $\delta_{LE}/a \approx 0.033$)

Distance between the end of the nozzle and the elastic panel

Inlet BC
$M_{\infty} = 2.0$

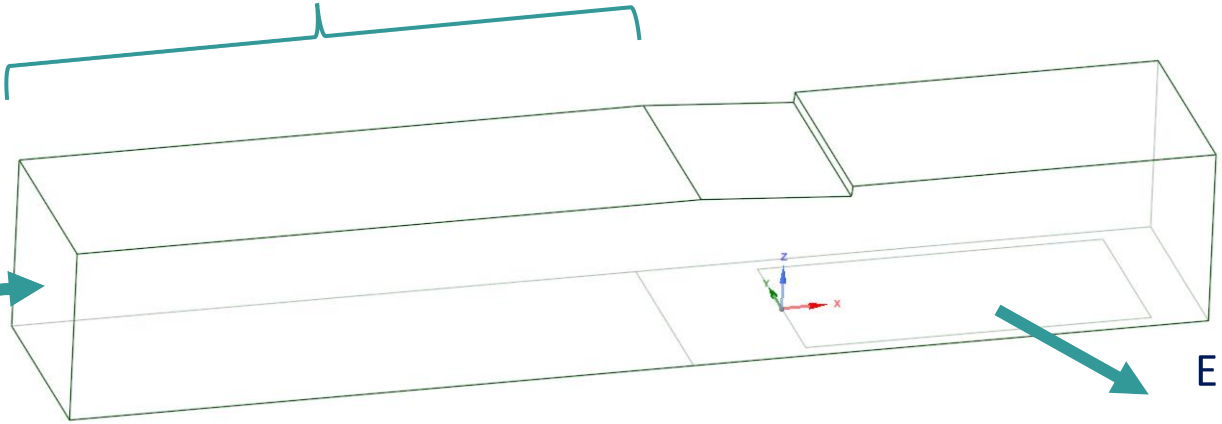

Outlet BC

Enforced motion only on the “elastic panel”

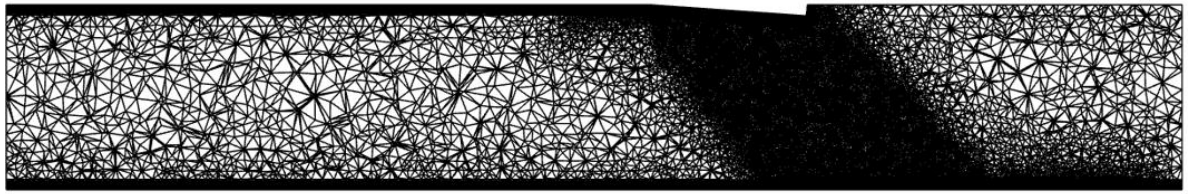

Inflation layer on the lower and upper (pre-wedge/wedge) walls

DLTA with a Viscous Shock Impingement

$\theta = 4^{\circ}$ wedge shock configuration

$\Delta T = 15$ K
$y^{+} = 1$

Mean & SDT deformation
(at ¾ of the panel length)

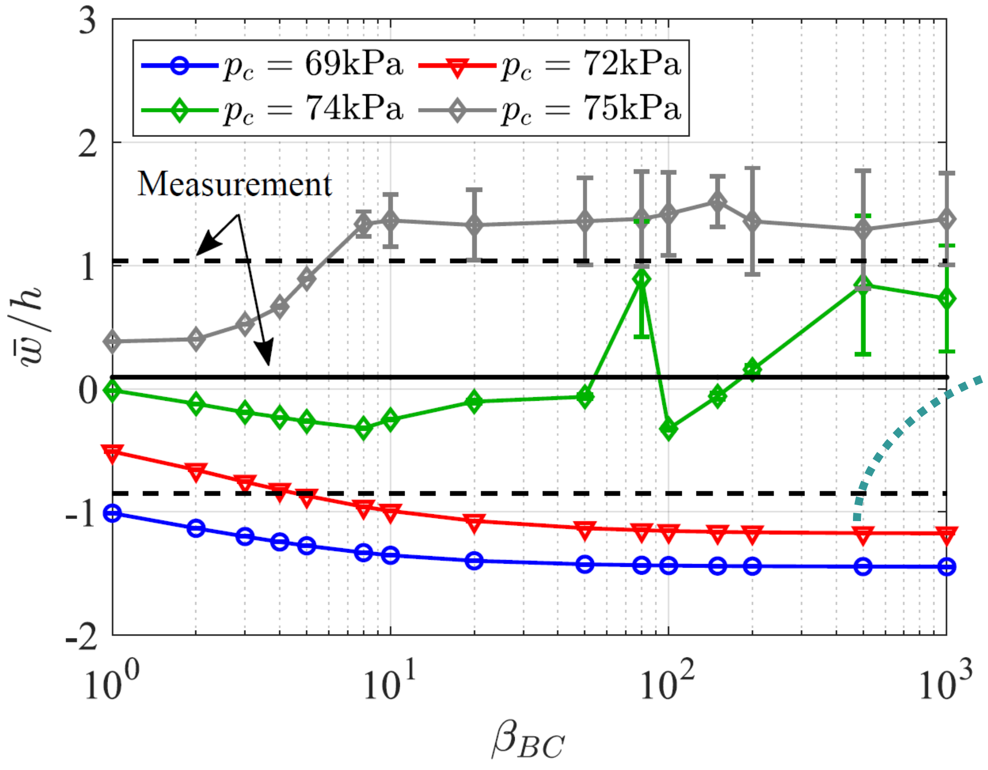

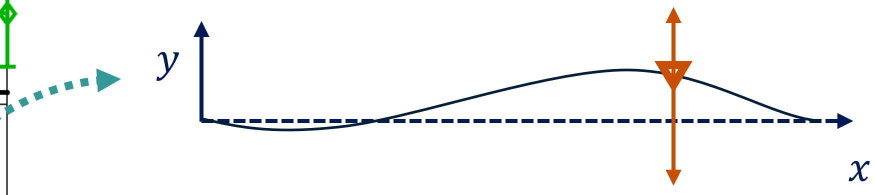

Wind Tunnel Setting

p_c (kPa)	ΔT (K)
68.9	13.3

Duke

DLTA with a Viscous Shock Impingement

$\theta = 4^{\circ}$ wedge shock configuration

$\Delta T = 15$ K
$y^{+} = 1$

Mean & SDT deformation
(at ¾ of the panel length)

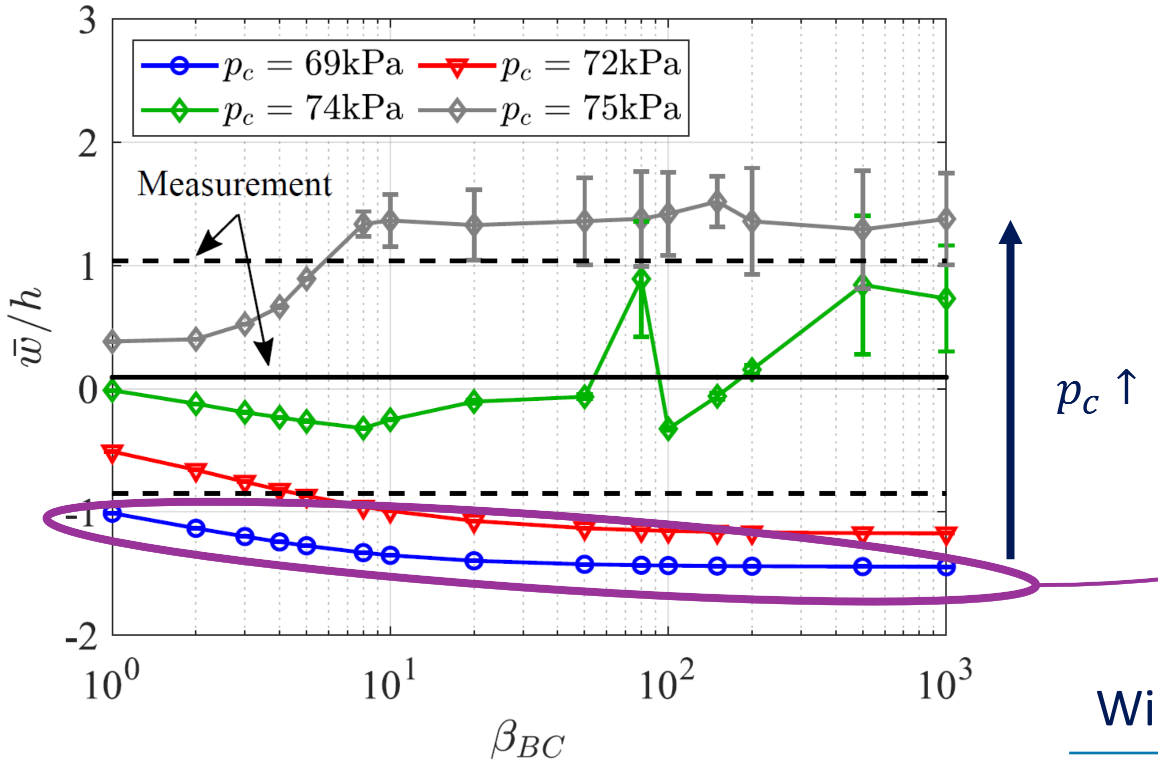

Similar to the wind tunnel setting

Wind Tunnel Setting

p_c (kPa)	ΔT (K)
68.9	13.3

Duke

DLTA with a Viscous Shock Impingement

$\theta = 4^{\circ}$ wedge shock configuration

$\Delta T = 15$ K
$y^{+} = 1$

Mean & SDT deformation
(at ¾ of the panel length)

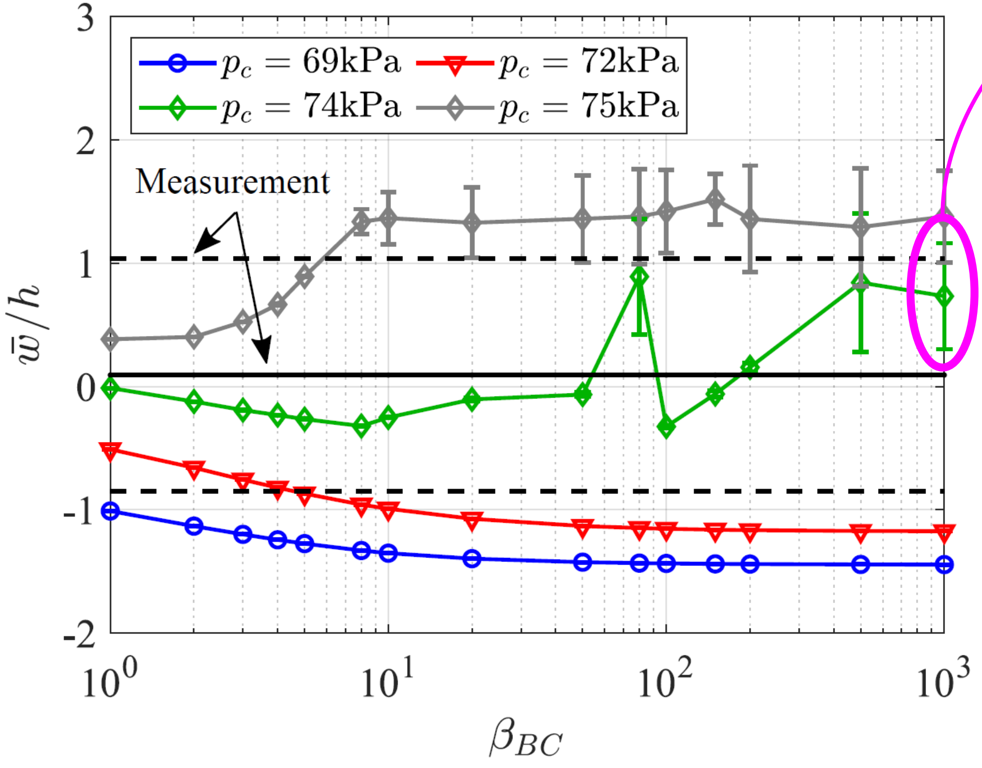

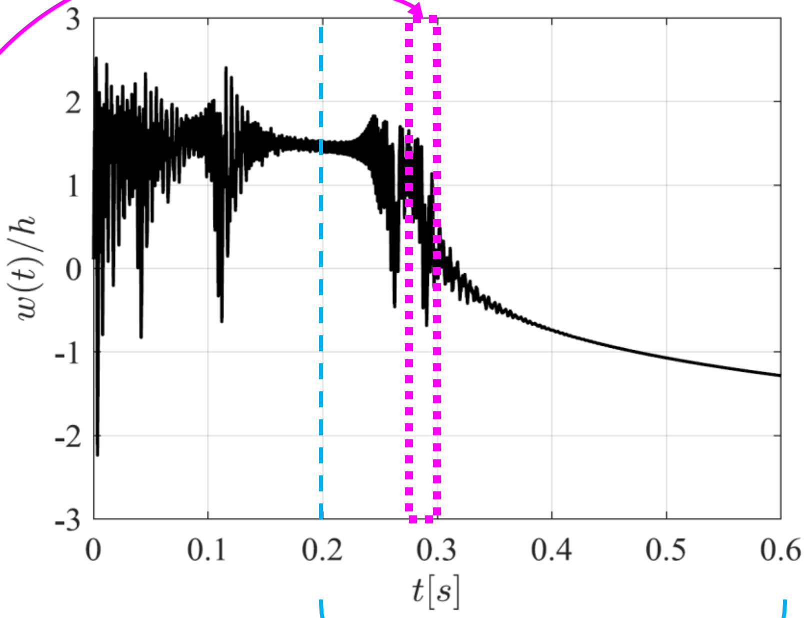

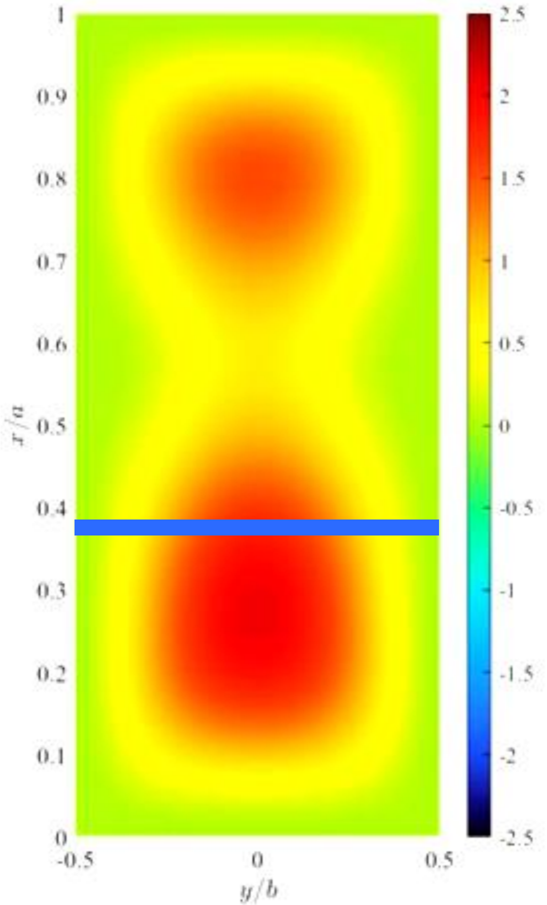

Flow Field

Wind Tunnel Setting

p_c (kPa)	ΔT (K)
68.9	13.3

Duke

Shock Impingement Aerodynamic Properties

Steady Solution

Local Mach number

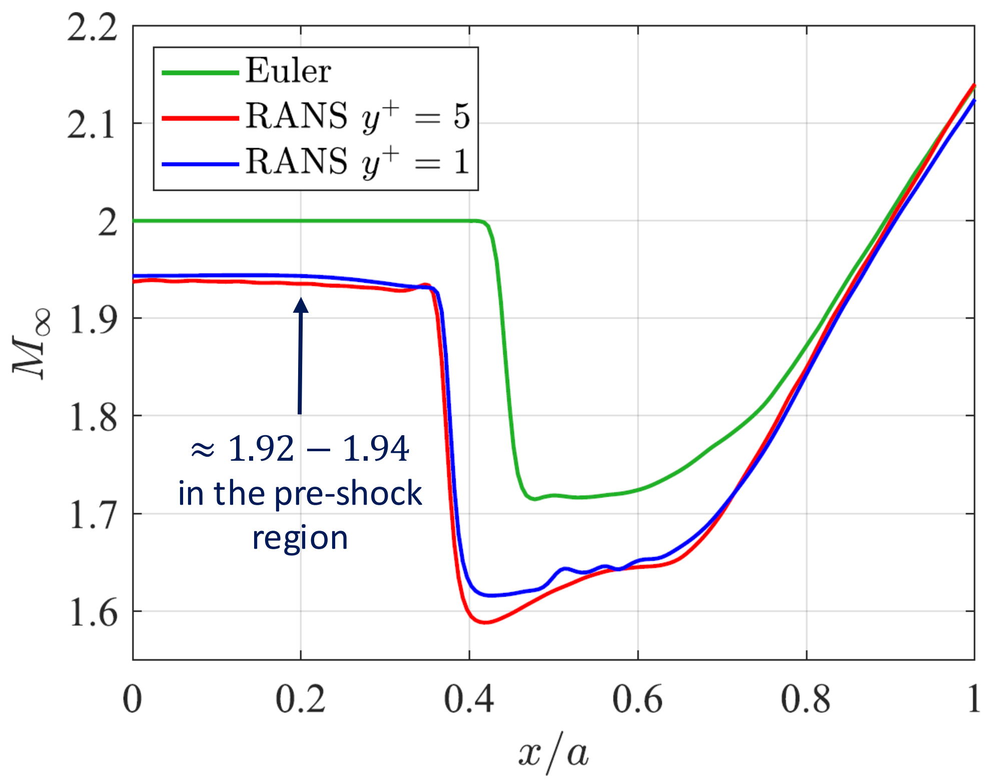

Flow more likely to cause structural instability

Static pressure

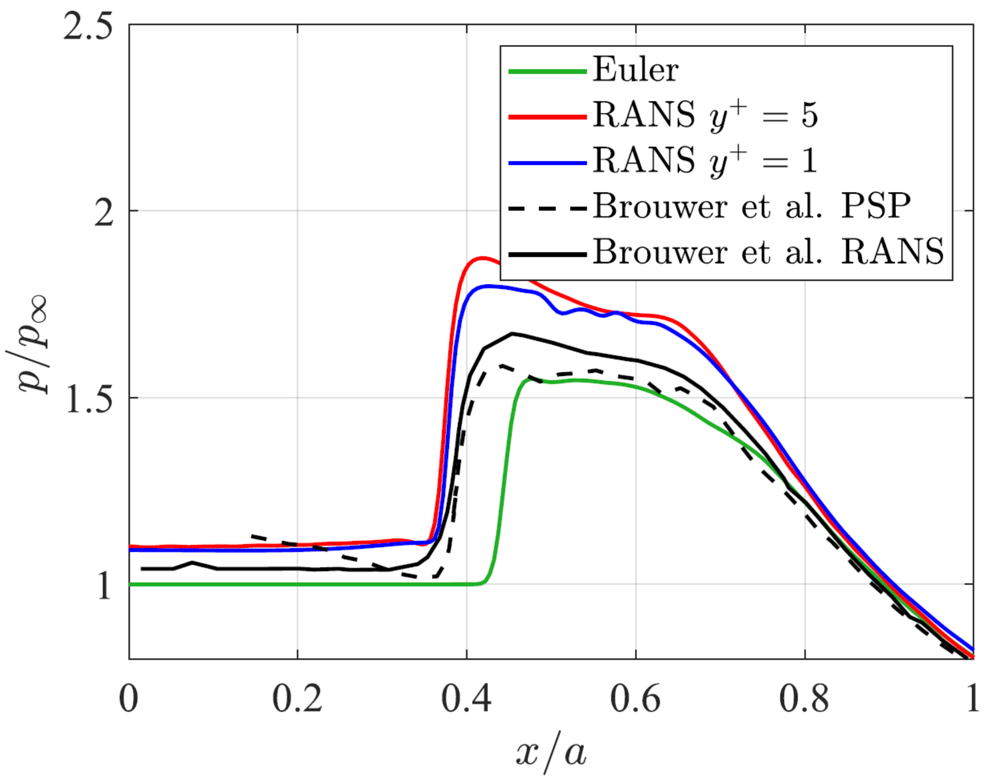

Panel stiffened by the Δp effect

Shock Impingement Aerodynamic Properties

Steady Solution

Static pressure differential

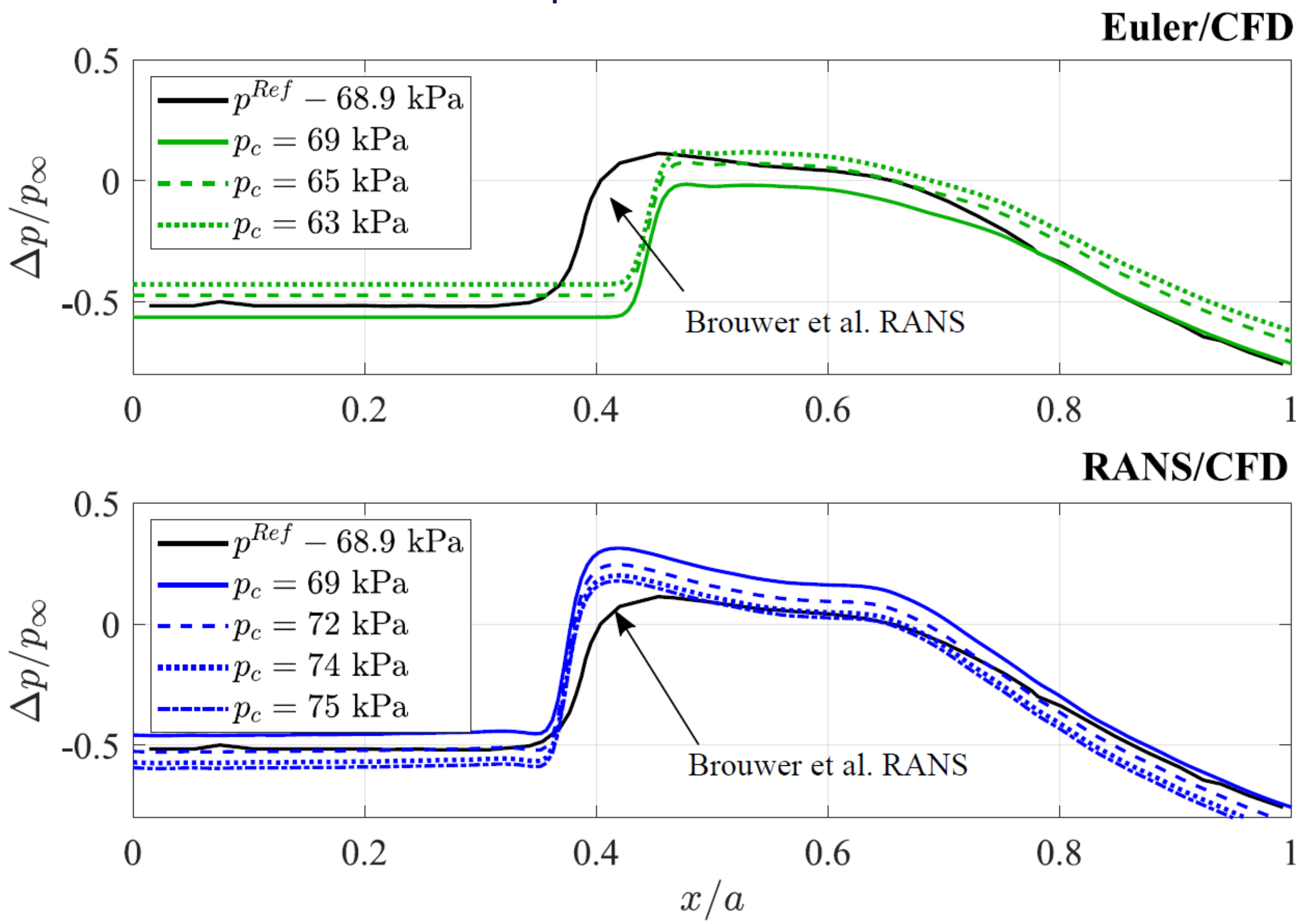

Panel stiffened by the Δp effect

Conclusion

- A range of aerodynamic models has been considered including Linear Piston Theory and Full Potential Flow for the no-shock case, and Euler and RANS/DLTA for the shock impingement case.
- For the RC-19 configuration **the results are particularly sensitive to the pressure differential, thermal stress (which leads to buckling) and the in-plane as well as out of plane boundary support conditions** for the plate.
- **Results for flutter and LCO of the RC-19 experiment are not particularly sensitive to the aerodynamic model**, with the key exception that when using the DLTA/CFD method, the steady solution for the shock location/magnitude can present indirect implications in the LCO prediction.

The computational models agree with the observations from experiments **on the essentials of the physical phenomena** e.g. buckling, flutter and limit cycle oscillations.

There is broad quantitative agreement between computations and experiments, given the sensitivity of the results to a wide range of parameters.

Duke

Correlation of Mathematical Model with AFRL RC-19 Aerothermoelastic Experiment Including an Impinging Shock

AIAA AVIATION Forum 2025

Luisa Piccolo Serafim and Earl Dowell – Duke University

Kirk Brouwer – AFRL, Wright-Patterson AFB

July 22, 2025 | Las Vegas, NV

Duke

Back-Up Slides

Duke

Δp *vs.* Natural Frequency: FEM *vs.* β_{BC} definition

$\Delta T = 0$
$U_\infty = 0$

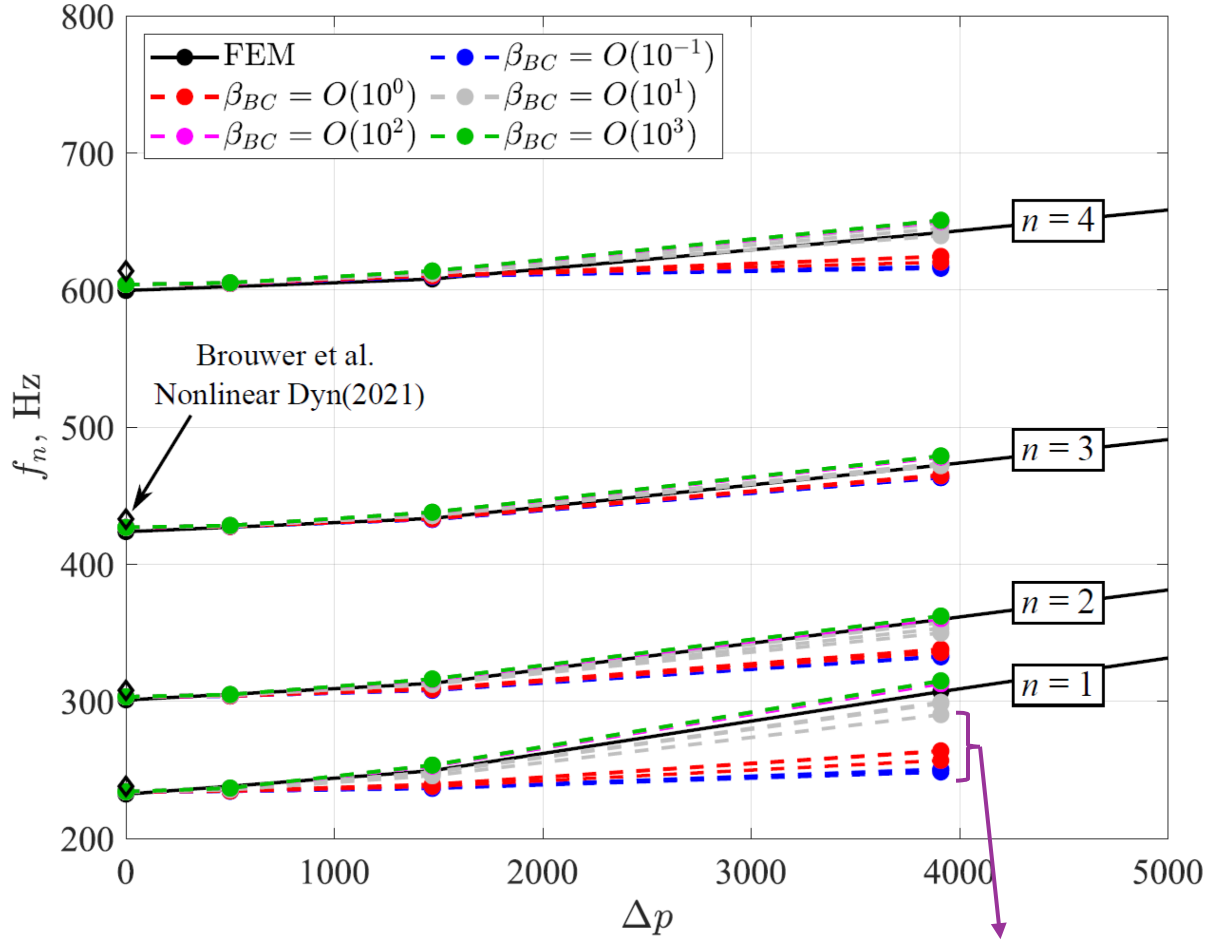

Plots include results for the symmetric ($\beta_{BC,x} = \beta_{BC,y}$)and asymmetric ($\beta_{BC,x} \neq \beta_{BC,y}$) in-plane stiffness, but they are roughly the same in all cases

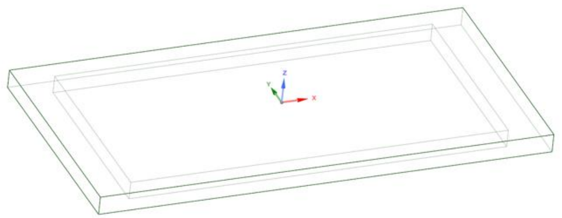

0.305×0.152×0.0127 m block of AISI 4140 alloy steel with a machined pocket, leaving the thin panel (elastic structure)

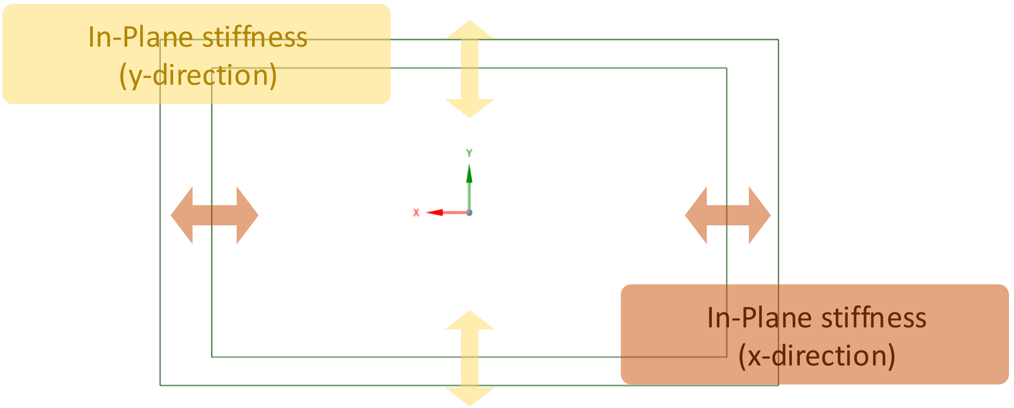

Expected range for the RC-19 conf. :

$O(10^1) < \beta_{BC} < O(10^2)$

Duke

Experimental Study Case: AFRL/SD RC-19 Wind Tunnel Section

Additional Considerations: Temperature Gradient ΔT

Thermally Buckled Condition

thermal loads (gradients) leading to compressive stresses and buckling deformation

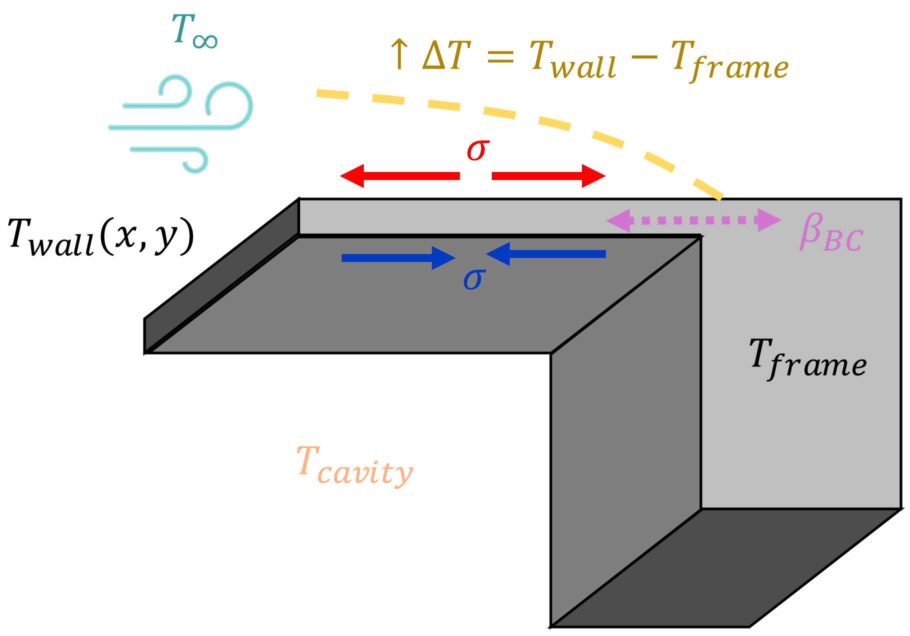

Piccolo Serafim et al. JFS (2023)

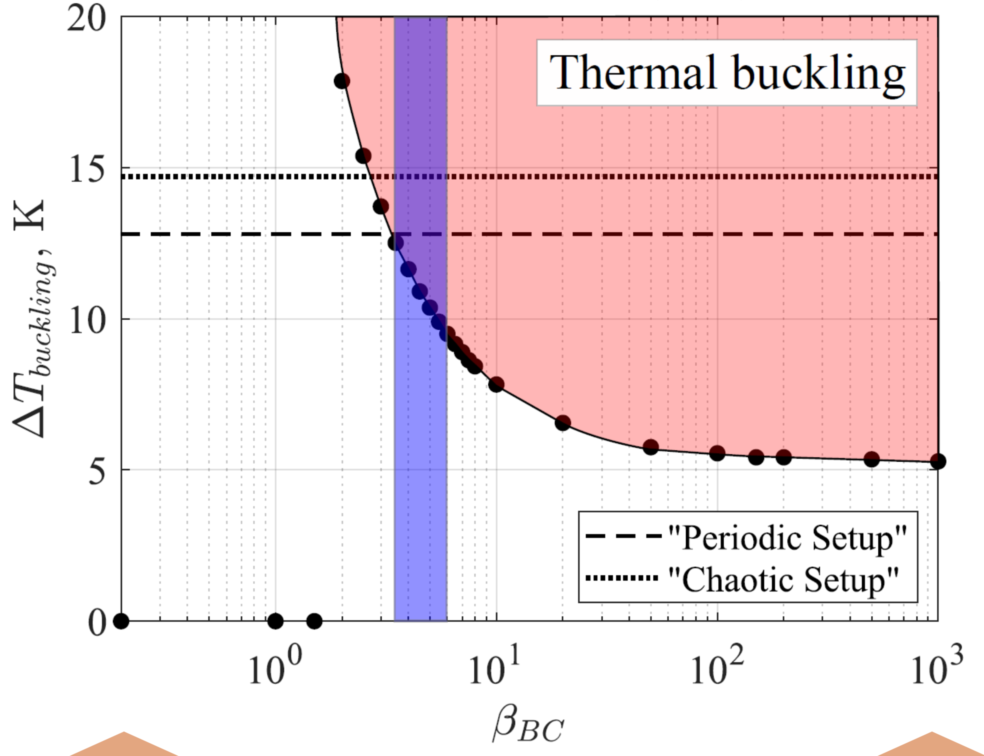

Free edge displacement
↓
No buckled condition

No edge displacement
↓
Buckled condition

Experimental Study Case: AFRL/SD RC-19 Wind Tunnel Section

Additional Considerations: acoustic response

Cavity Effect

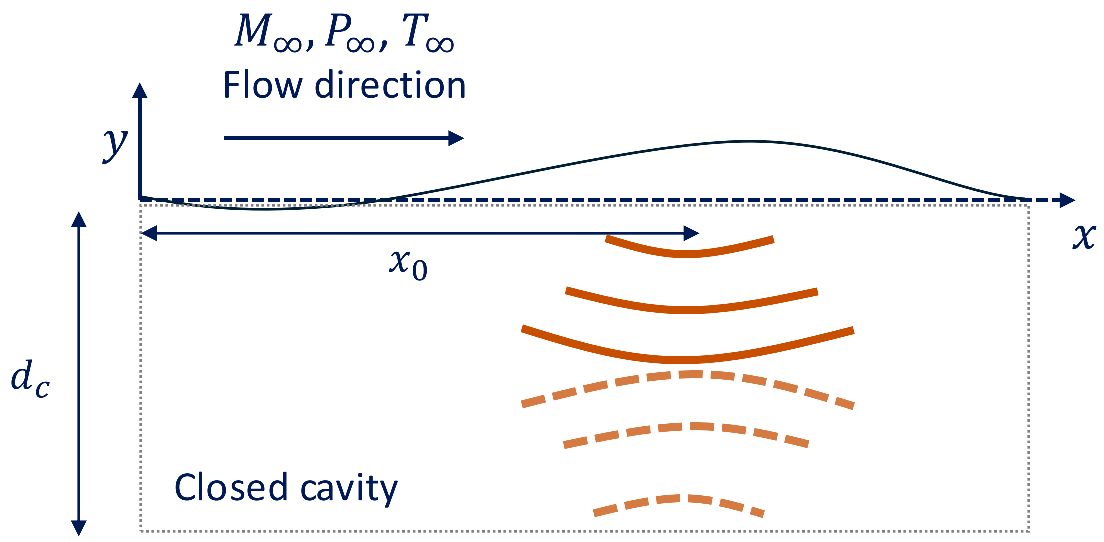

Cavity depth (d_c) exaggerated for illustration

Mean & SDT deformation

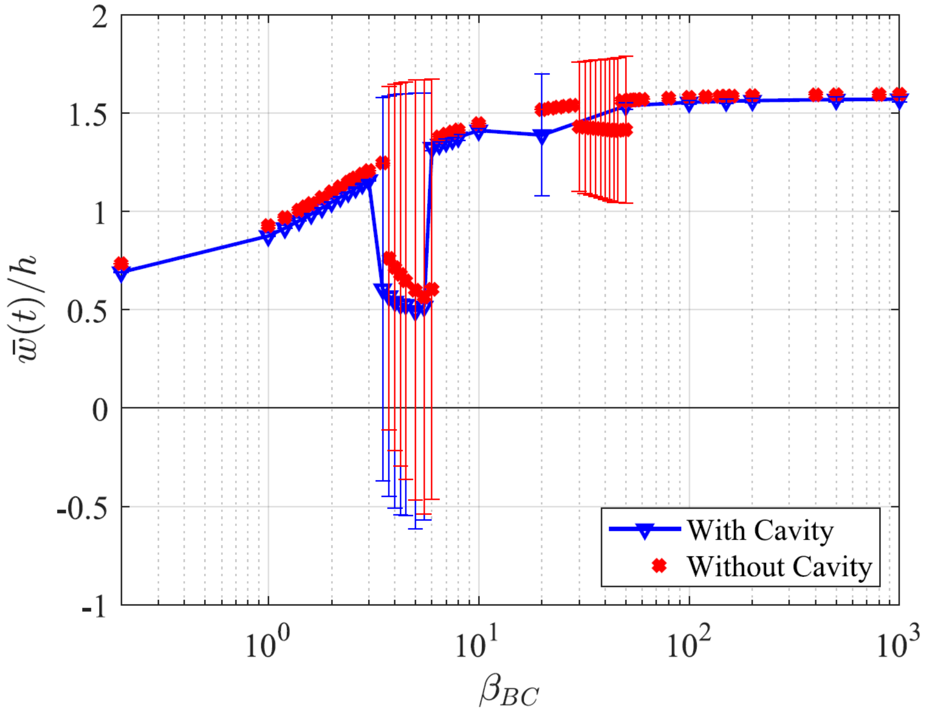

Piccolo Serafim et al. JFS (2023)

Duke

From Potential Flow to DLTA

Why we can neglect the $\int_0^t \dot{q}_m(\tau) I_{m,k}(t-\tau)d\tau$ term

$$Q_{mn}(t) = q_m(t)S_{mn} + \dot{q}_m(t)D_{mn} + \int_0^t q_m(\tau)H_{mn}(t-\tau)d\tau + \int_0^t \dot{q}_m(\tau)I_{mn}(t-\tau)d\tau$$

$$Q_{mn}(t) = q_m(t)S_{mn} + \dot{q}_m(t)D_{mn} + \int_0^t q_m(\tau)\left[H_{mn}(t-\tau) - \frac{dI_{mn}(t-\tau)}{d\tau}\right]d\tau + q_m(t)I_{mn}(0) - q_m(0)I_{mn}(t)$$

$$Q_{mn}(t) = q_m(t)S_{mn} + \dot{q}_m(t)D_{mn} + \int_0^t q_m(\tau)\underbrace{\left[H_{mn}(t-\tau) + \frac{dI_{mn}(t-\tau)}{dt}\right]}d\tau$$

$$H_{mn}(t-\tau) \gg \frac{dI_{mn}(t-\tau)}{dt}$$

Duke

ROM to include unsteady aerodynamics into the aeroelastic solution

Knowing …

… the linear relationship seen in the Full Potential Theory, …

$$Q_n(t) = q_m(t)S_{mn} + \dot{q}_m(t)D_{mn} + \int_0^t q_m(\tau)H_{mn}(t-\tau)d\tau + \int_0^t \dot{q}_m(\tau)I_{mn}(t-\tau)d\tau$$

… that if we run a CFD solution for a known mesh deformation, we obtain the pressure field as a function of space and time, …

$t = 0$ $\quad$ $t = \Delta t$

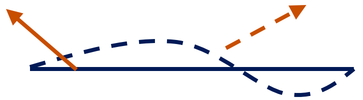

Known deformation (input) ⟶ Known pressure field (output)

… and that we can use the general definition of GAF for on the CFD known pressure field…

$$Q_{mn}^{CFD}(t) = \int_0^b \int_0^a \frac{p_{CFD,m}(x,y,t) - p_\infty}{\rho_\infty U_\infty^2} \psi_n(x,y)dxdy$$

… we can define a linear expression for the GAF where we obtain the characteristics matrices A_{mn}, B_{mn}, and $E_{mn}(t)$ for an arbitrary surface deformation ($q_m(t)$ and $\dot{q}_m(t)$)

$$Q_{mn}^{CFD}(t) = q_m(t)A_{mn} + \dot{q}_m(t)B_{mn} + \int_0^t q_m(\tau)E_{mn}(t-\tau)d\tau$$

Dynamically Linearized Time-domain Approach (DLTA)

ROM to include unsteady aerodynamics into the aeroelastic solution

Step change in the CFD domain for each ψ_{mn} …

… in the panel deformation:

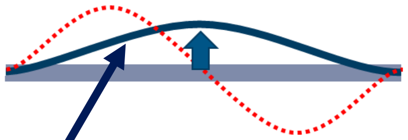

$$Q_{mn}^{CFD}(t) = \overset{=\begin{cases}0, t<0\\ \chi, t\geq 0\end{cases}}{\cancel{q_m(t)}}A_{mn} + \overset{=0}{\cancel{\dot{q}_m(t)}}B_{mn} + \int_0^t \overset{=\begin{cases}0, t<0\\ \chi, t\geq 0\end{cases}}{\cancel{q_m(\tau)}}E_{mn}(t-\tau)d\tau$$

The panel deformation/velocity is a mode shape (input). Ex: $mn = (1,1)$ mode

Resulting pressure field (output)

$$Q_{mn}^{CFD}(t) = \iint \frac{\boxed{\Delta p_m(x,y,t)}}{\rho_\infty U_\infty^2}\psi_n(x,y)\,dxdy$$

… in the velocity of the panel deformation:

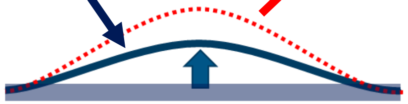

$$Q_{mn}^{CFD}(t) = \overset{=0,\,@\,t=0}{\cancel{q_m(t)}}A_{mn} + \overset{=\begin{cases}0, t<0\\ \chi, t\geq 0\end{cases}}{\cancel{\dot{q}_m(t)}}B_{mn} + \int_0^t \overset{=0,\,@\,t=0}{\cancel{q_m(\tau)}}E_{mn}(t-\tau)d\tau$$

Once A_{mn}, B_{mn}, and $E_{mn}(t)$ are obtained, we can reconstruct the Generalized Aerodynamic Force inside the Aeroelastic Solver for any arbitrary panel deformation $(q_m(t), \dot{q}_m(t))$

$$\boxed{Q_{mn}^{CFD}(t) = q_m(t)A_{mn} + \dot{q}_m(t)B_{mn} + \int_0^t q_m(\tau)E_{mn}(t-\tau)d\tau}$$

Duke

Including the Shock Wave Effect

Ansys 2022 R1

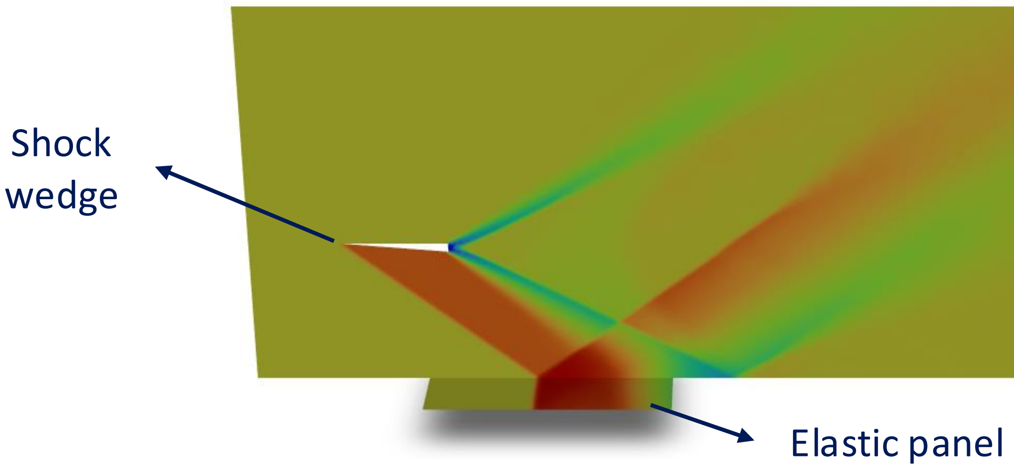

$$\Delta p = \underbrace{\frac{p_{CFD} - p_{steady}}{\chi}}_{\text{“Scalable pressure”}} + \underbrace{\left(p_{steady} - p_{\infty}\right)}_{\text{Shock Profile}}$$

“Scalable pressure” → Unsteady aerodynamics depended on the panel deformation

Shock Profile → Static pressure <u>always</u> acting on the panel surface

p_{steady} → steady pressure distribution (with the shock wave)

p_{CFD} → unsteady pressure distribution (with the shock wave AND the step change)

Duke

Mathematical/Computational Modeling

Nonlinear Aeroelastic Solver

Set Boundary Conditions

- p_C fixed
- ΔT fixed
- ICs
- Flow parameters

Compute Structural Matrices

Compute Aerodynamic Matrices

Solve ODE in terms of the generalized coord.

Flat Panel

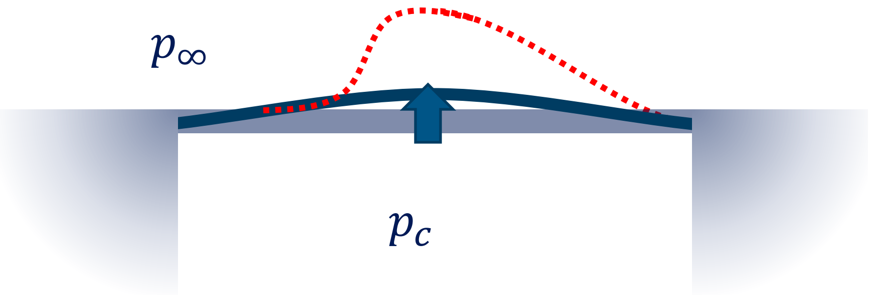

IC: small perturbation at the first mode shape
Cavity pressure
Flow field + shock impingement

Duke

Shock Impingement Aerodynamic Properties

Steady Solution

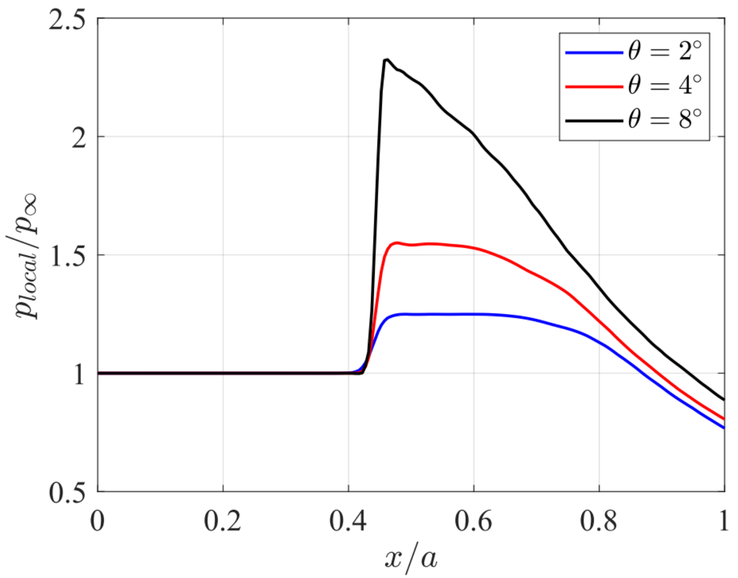

Panel stiffened by the Δp effect

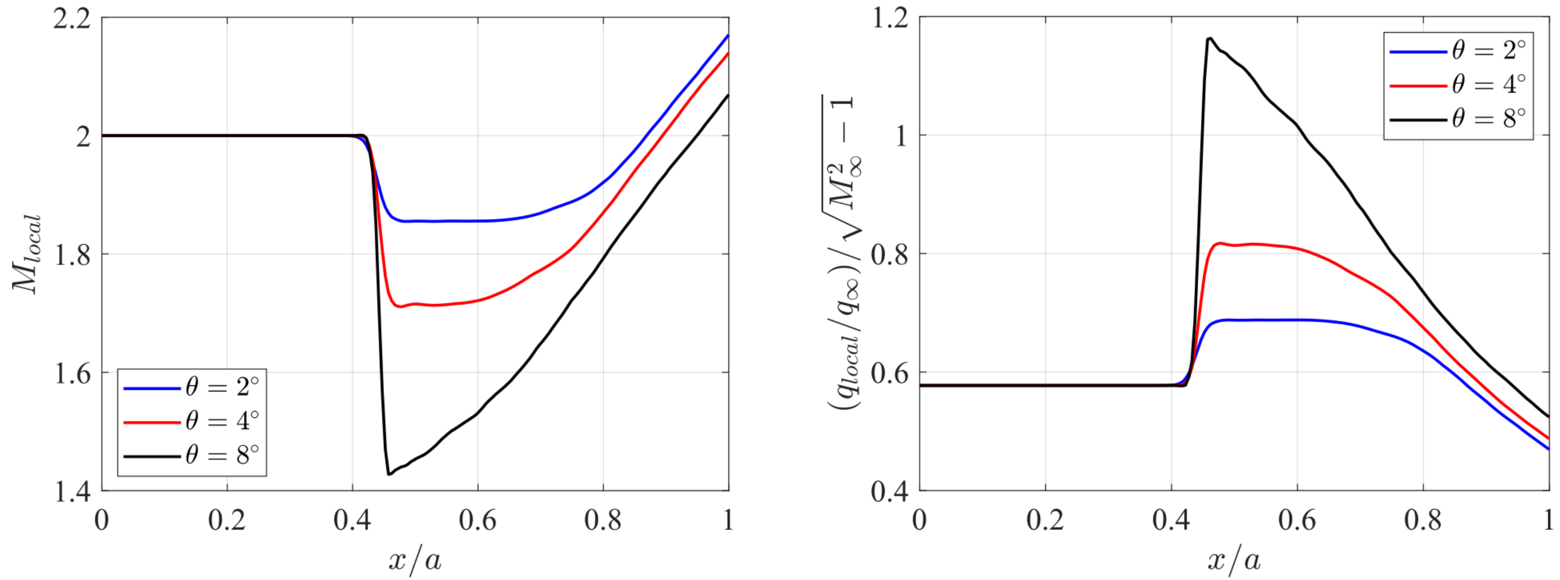

Flow more likely to cause structural instability

Duke

Piccolo Serafim and Dowell. IFASD (2024)

Shock Impingement in Time

Unsteady pressure field implications on the $E_{mn}(t)$ matrix

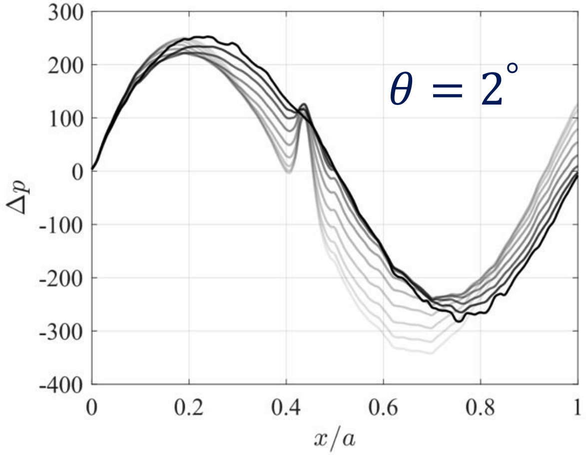

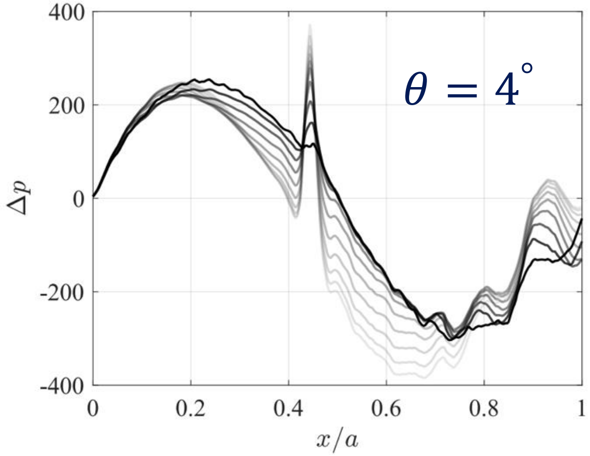

$\Delta p = p_{local}(x, y, t) - p_{steady}(x, y)$ <u>vs.</u> panel chord at many time step

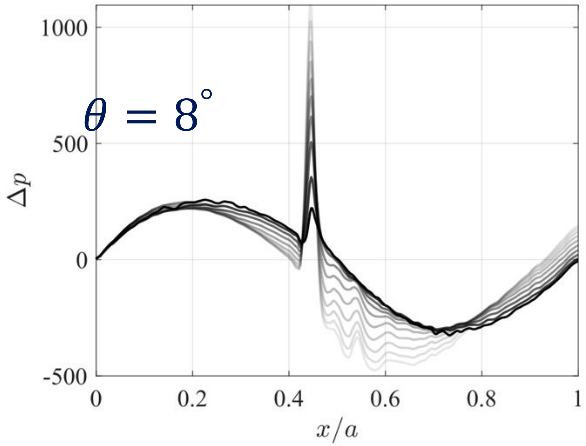

$E_{1,1}(t)$ vs. nondimensional time

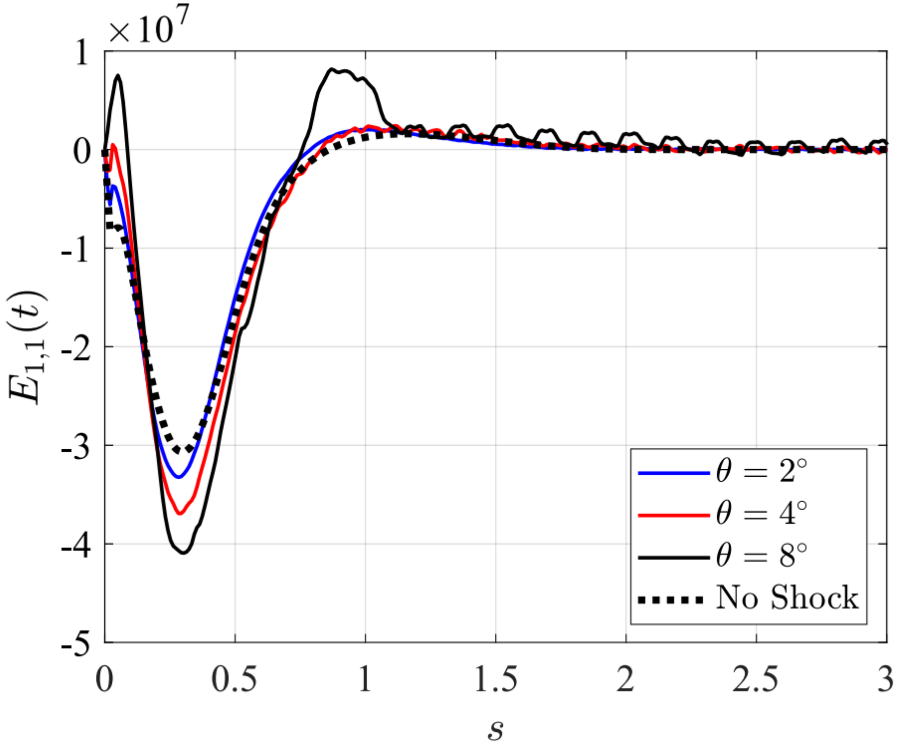

Time lapse for the pressure distribution over the panel length, at mid-span, given a step change in the first mode shape of the panel

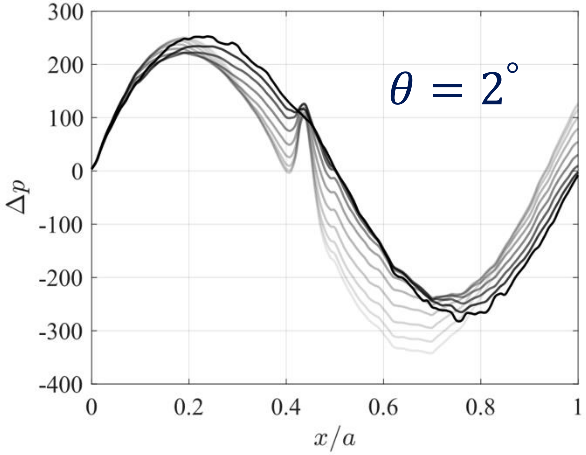

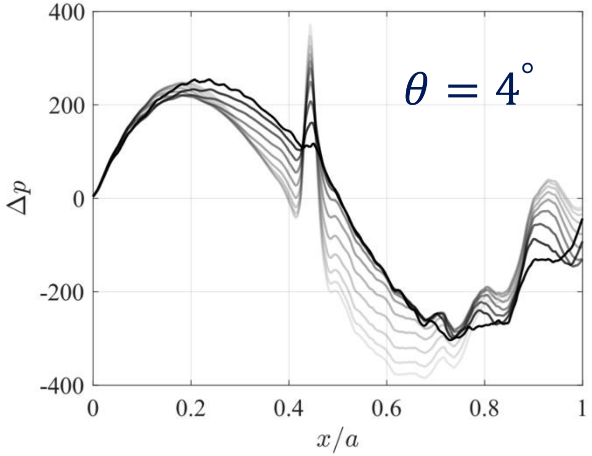

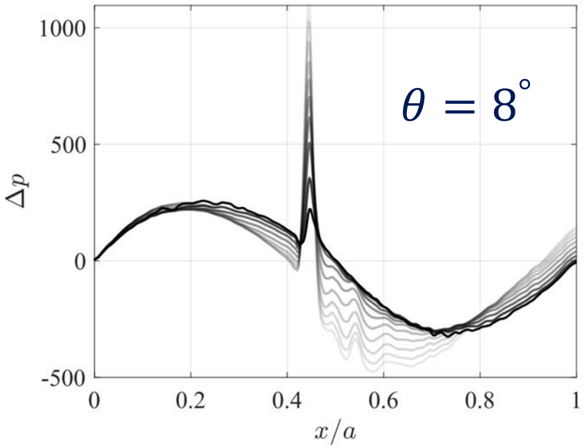

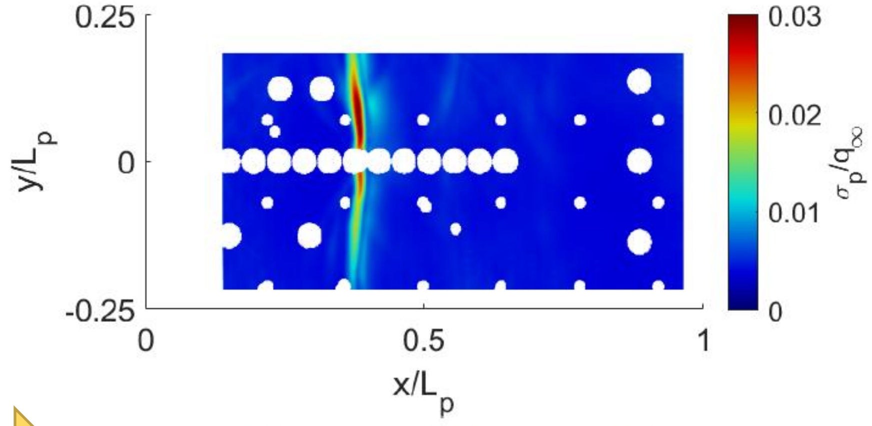

(a) Pressure sensitive paint (PSP).

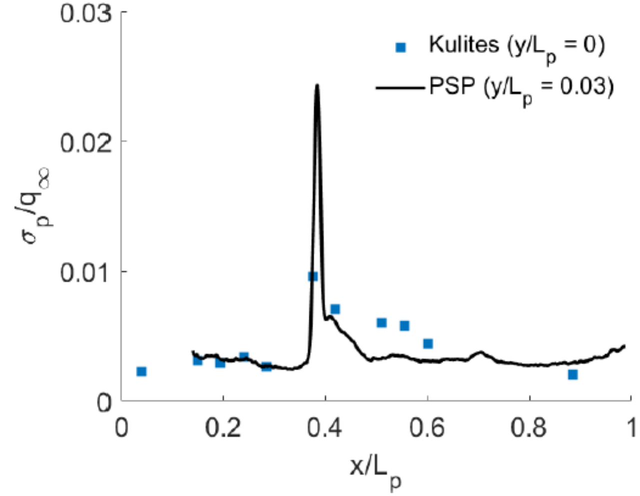

(b) Comparison between PSP and Kulites.

Brouwer et al. AIAA AVIATION Forum (2023)

Duke

Nonlinear Aeroelastic Model

Updated Equation of Motion

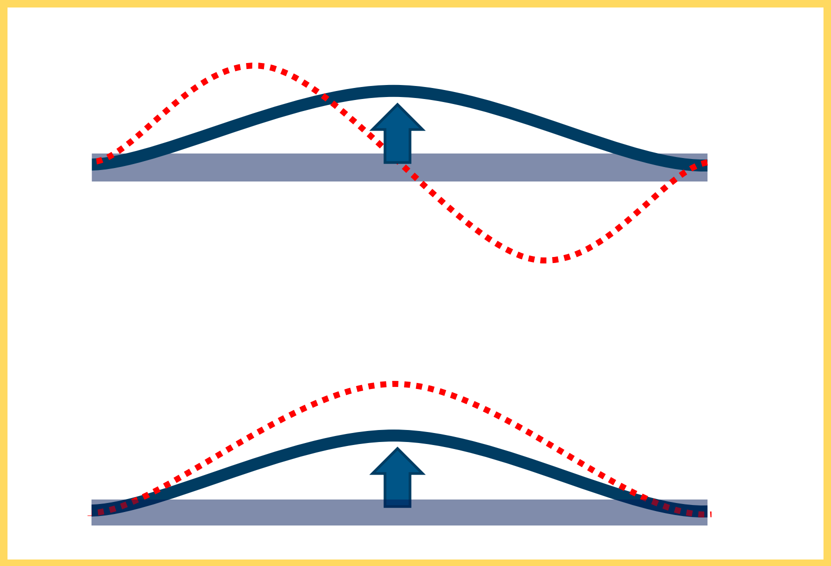

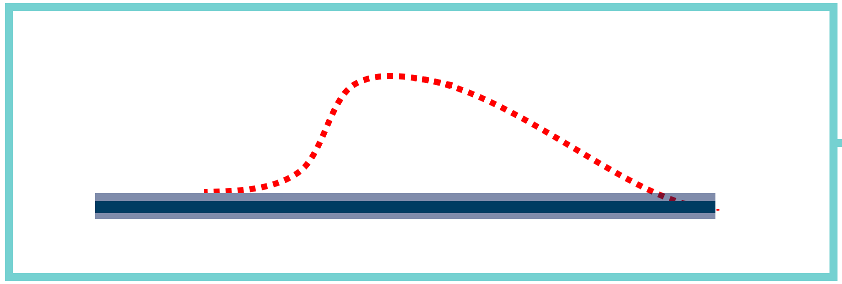

$$\underbrace{M_{mn}\ddot{q}_n(t) + C_{mn}\dot{q}_n(t) + G^{(2)}_{mn}q_n(t)}_{\text{Linear plate model}} +$$

$$\underbrace{D^{(2)}_{mnrp}q_n(t)q_r(t)q_p(t)}_{\text{NL structural stiffness}} +$$

$$\underbrace{Q^{Aero}_n(t)}_{\substack{\text{Unsteady Aerodynamics} \\ \text{(DLTA)}}} +$$

$$\underbrace{Q^{Shock}_n}_{\substack{\text{Steady shock} \\ \text{pressure}}} = 0$$

DLTA with an Inviscid Shock Impingement

Mean deformation

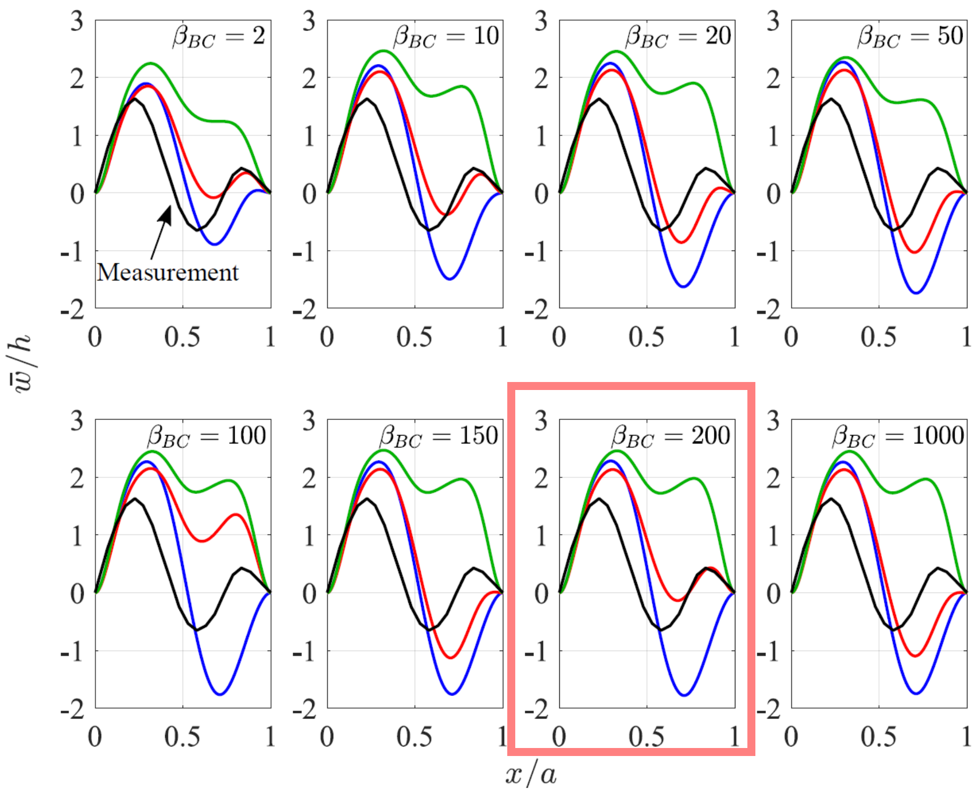

Standard deviation

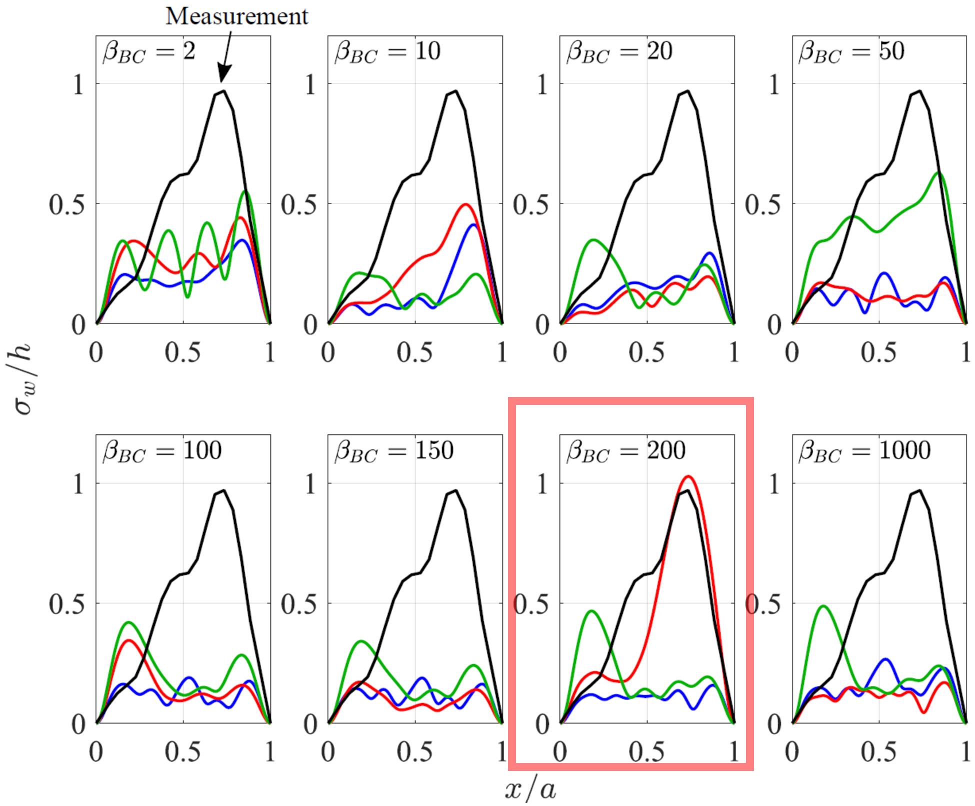

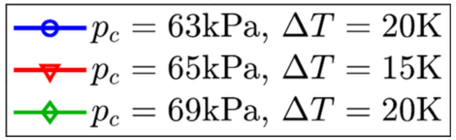

Nondimensional in-plane boundary stiffness

$$\beta_{BC} \equiv \frac{K_{BC}a}{Eh}$$

$\beta_{BC} \approx 0$: Free edge displacement

$\beta_{BC} \gg 0$: No edge displacement

Duke

(at ¾ of the panel length)

DLTA with an Inviscid Shock Impingement

Deformation in time

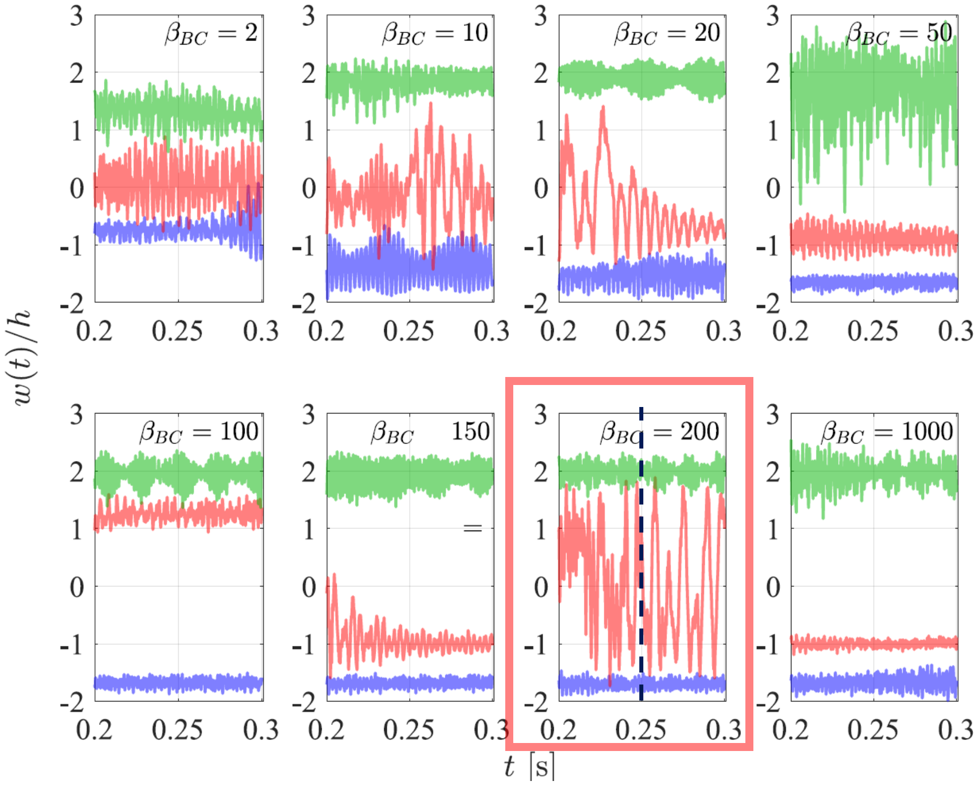

Standard deviation

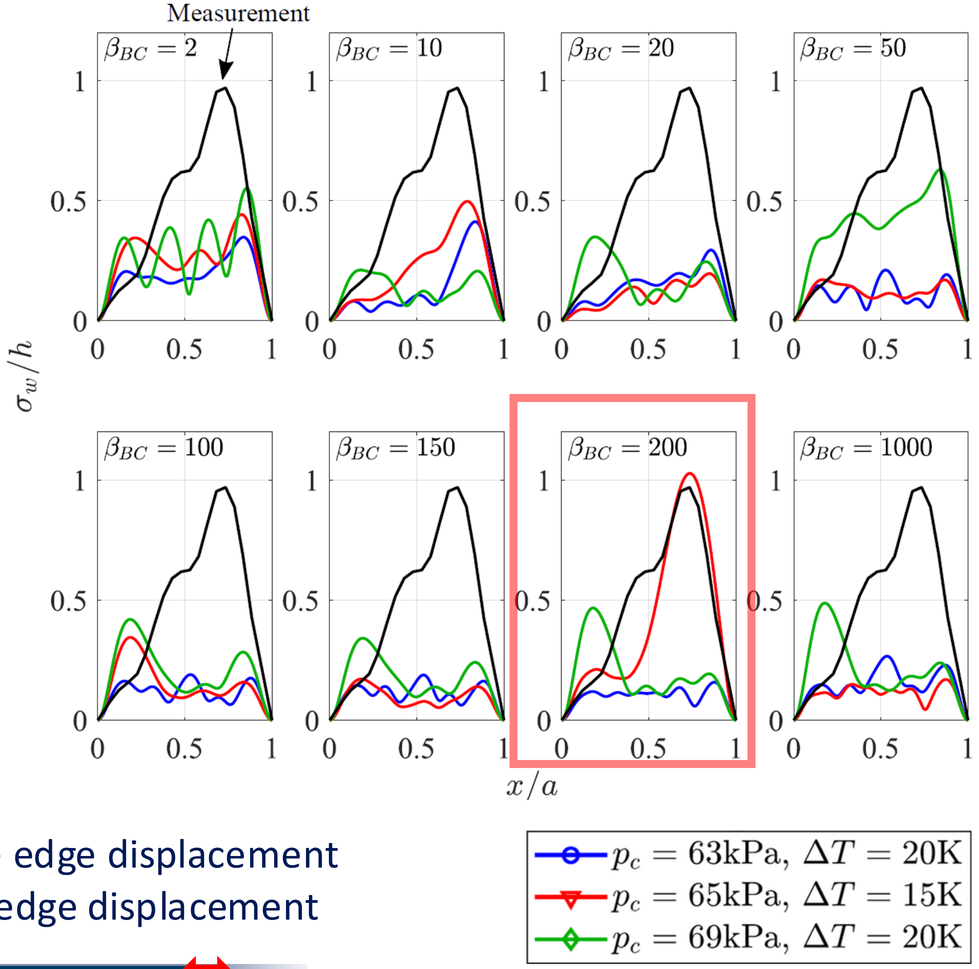

Nondimensional in-plane boundary stiffness

$$\beta_{BC} \equiv \frac{K_{BC}a}{Eh}$$

$\beta_{BC} \approx 0$: Free edge displacement

$\beta_{BC} \gg 0$: No edge displacement

Duke

DLTA with a Viscous Shock Impingement

$\Delta T = 15$ K
$y^+ = 1$

Mean deformation

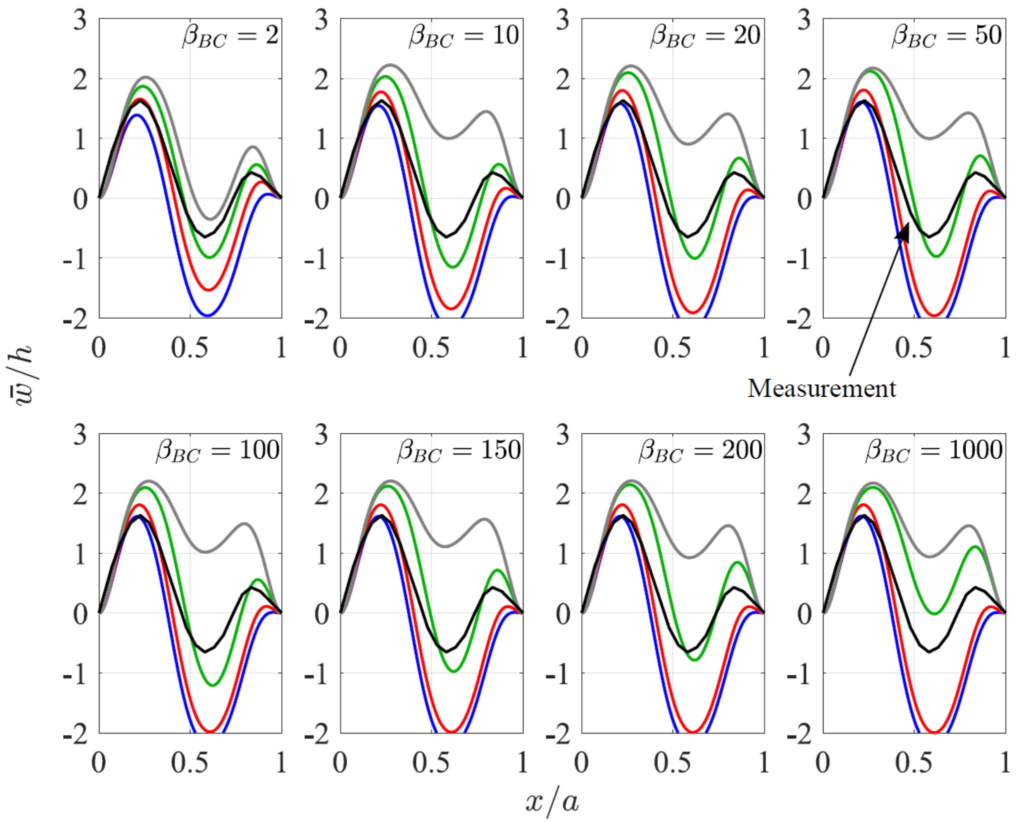

Standard deviation

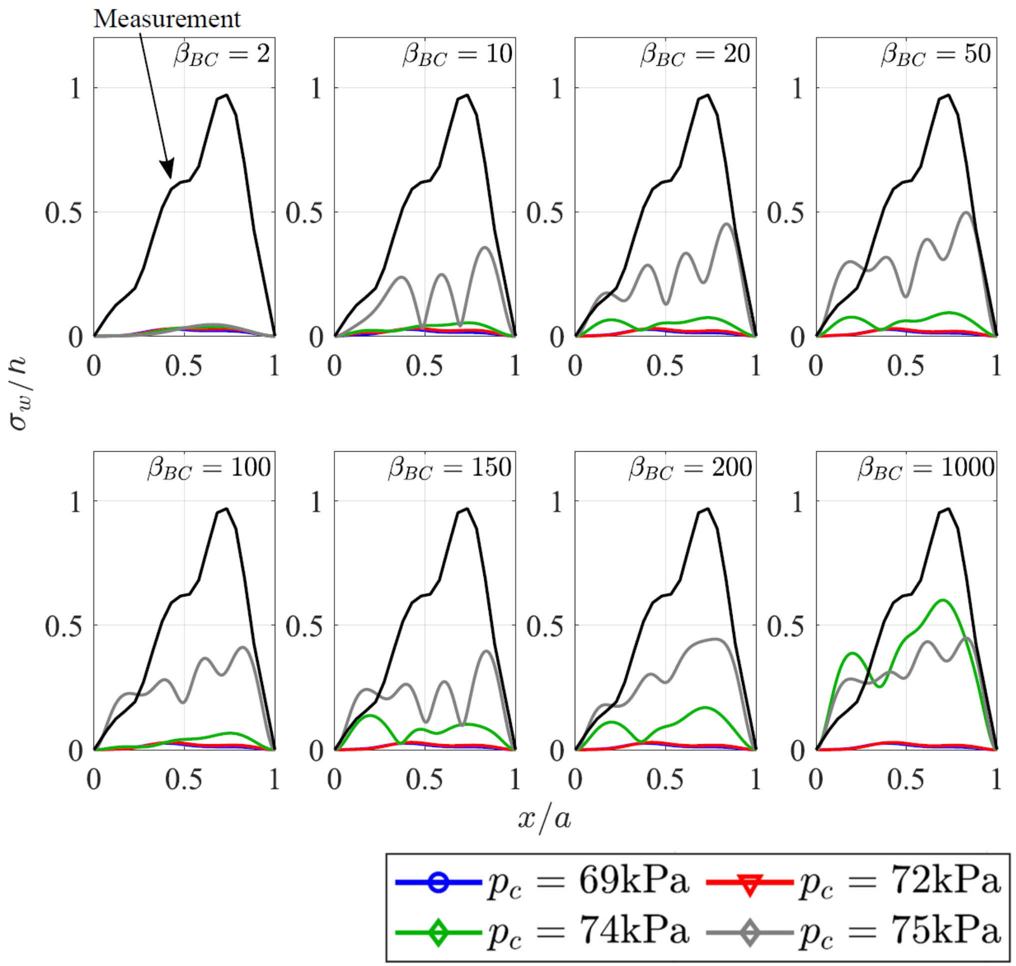

Duke

DLTA with a Viscous Shock Impingement

$\Delta T = 15$ K
$y^+ = 1$

Deformation in time

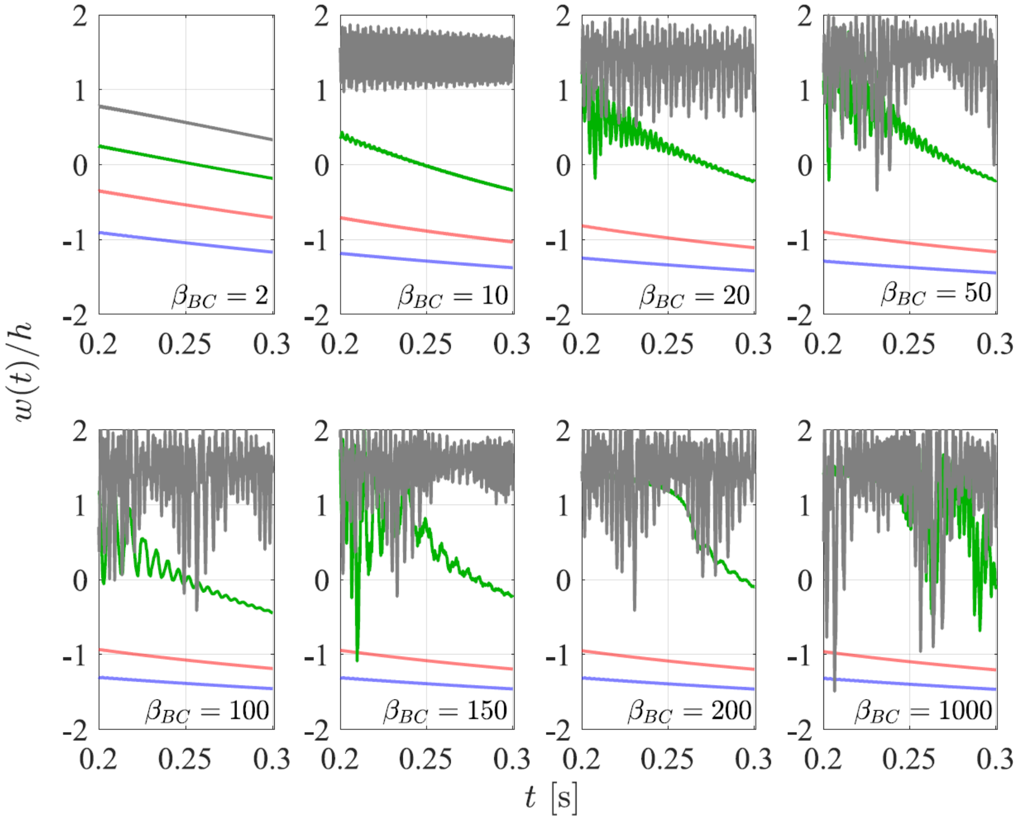

Standard deviation

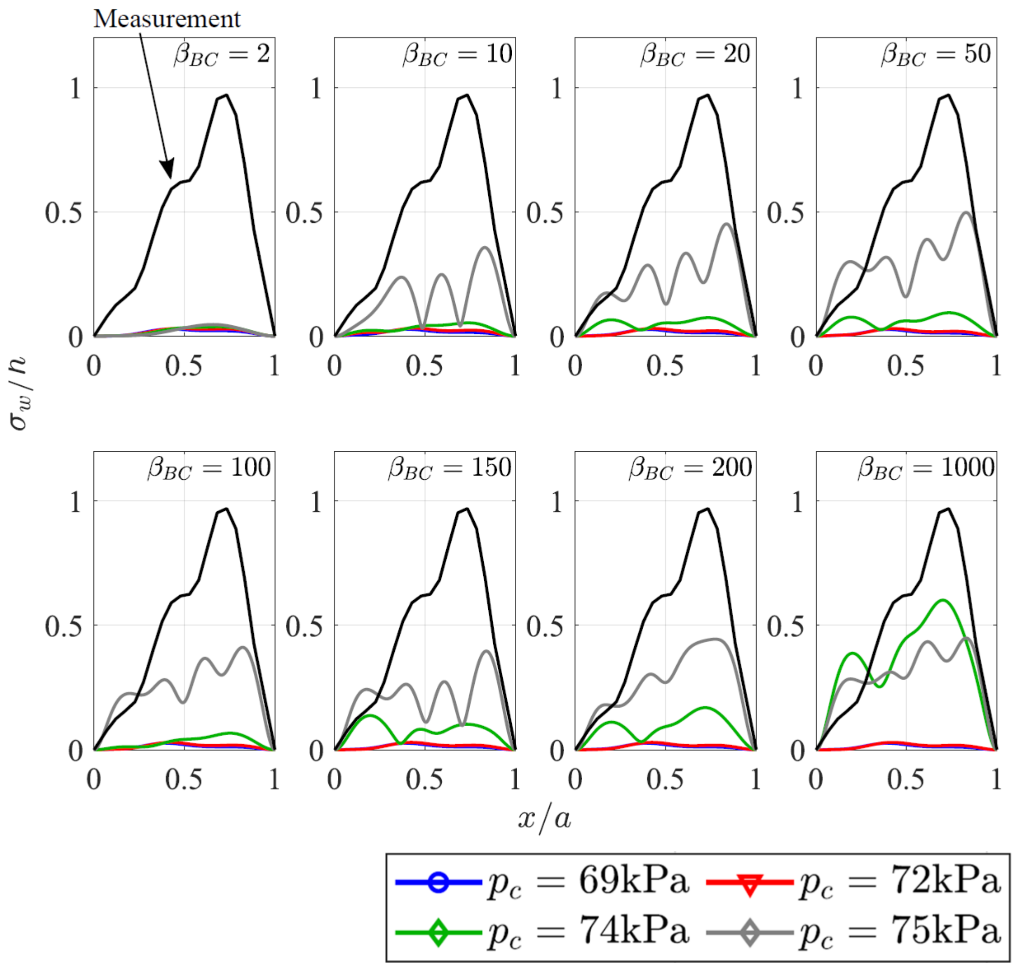

Duke

DLTA with a Viscous Shock Impingement

$\Delta T = 15$ K
$y^+ = 1$

Deformation in time

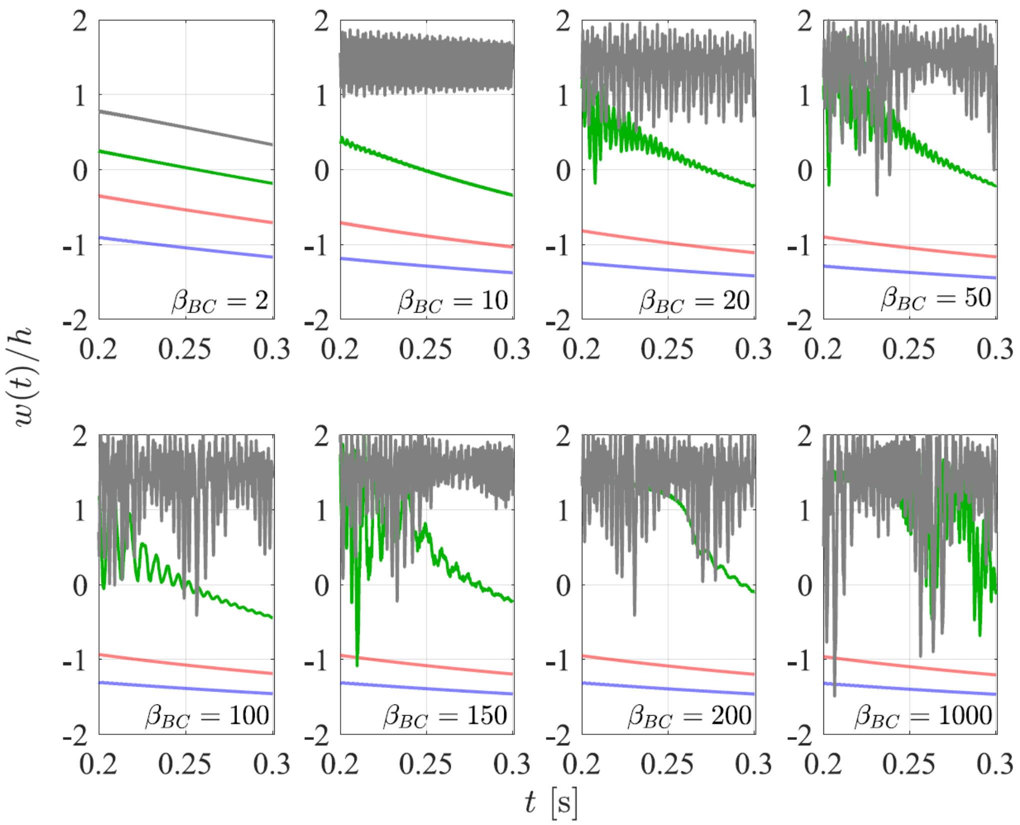

Mean deformation

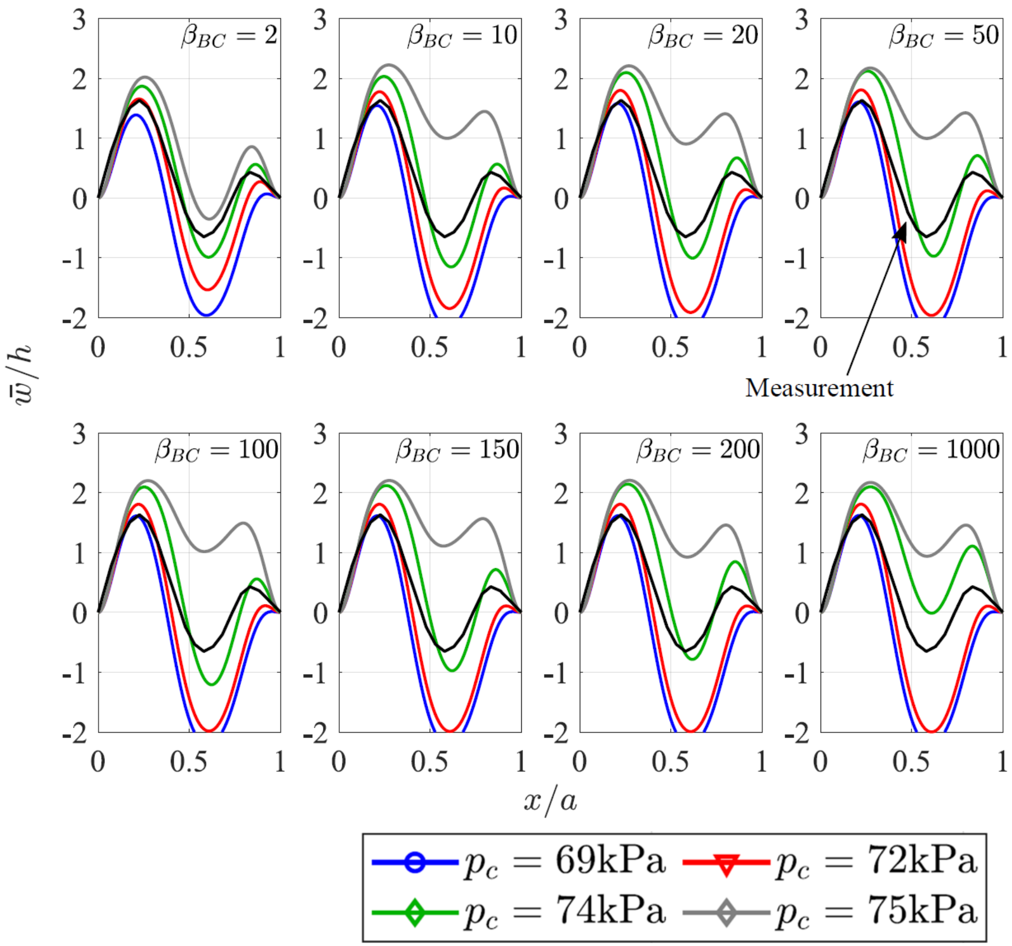

Duke

DLTA with a Viscous Shock Impingement

$\Delta T = 15$ K
$y^{+} = 1$

$\theta = 4^{\circ}$ wedge shock configuration

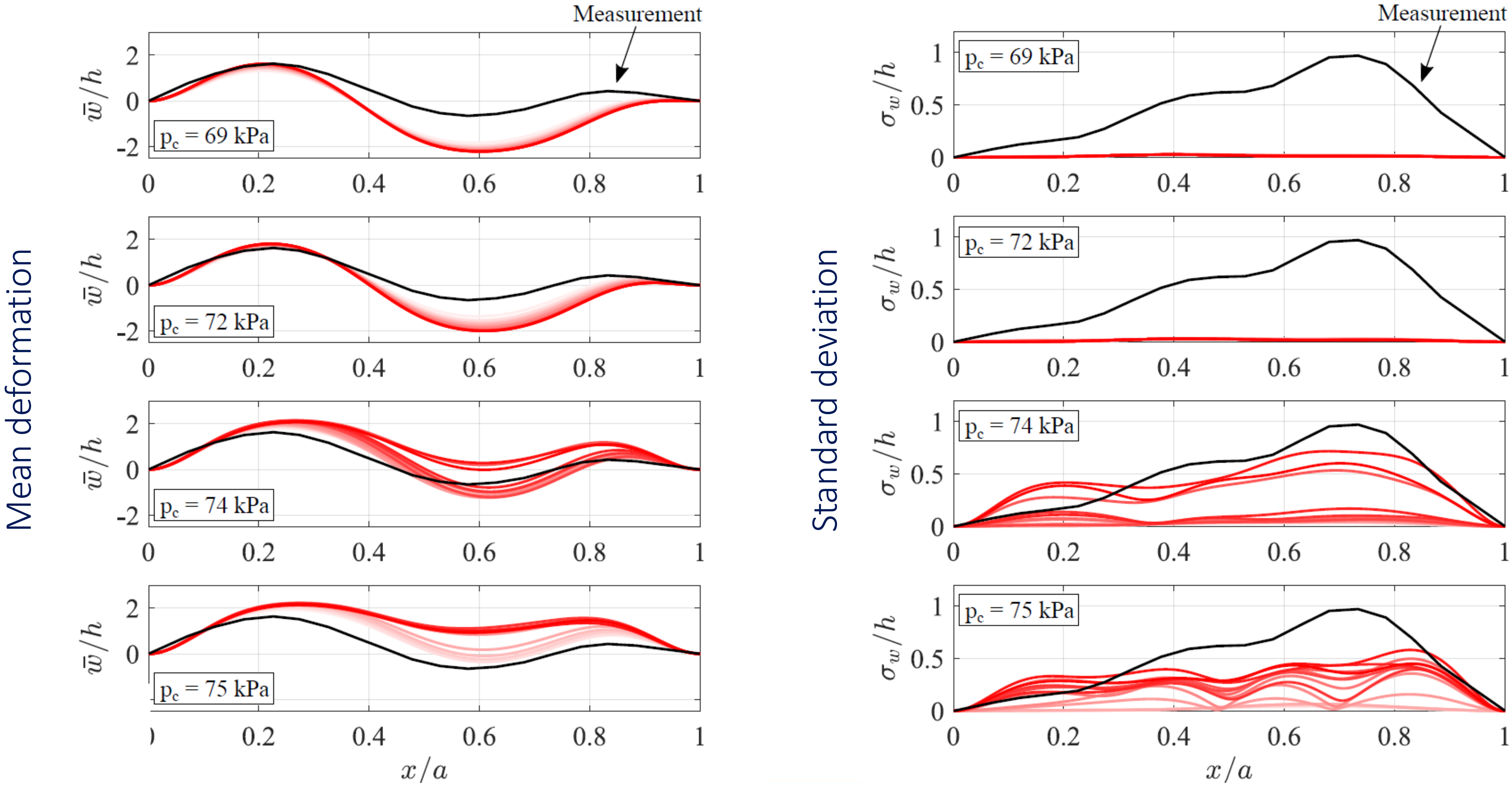

$\Delta T = 15$ K

DLTA with a Viscous Shock Impingement

$\theta = 4^{\circ}$ wedge shock configuration

Mean & SDT deformation

(at ¾ of the panel length)

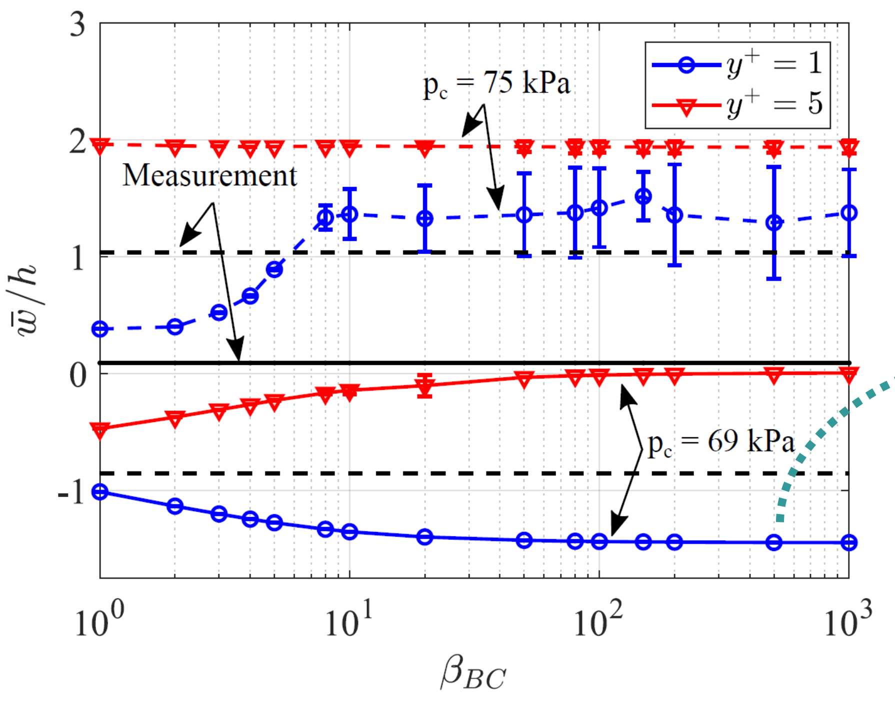

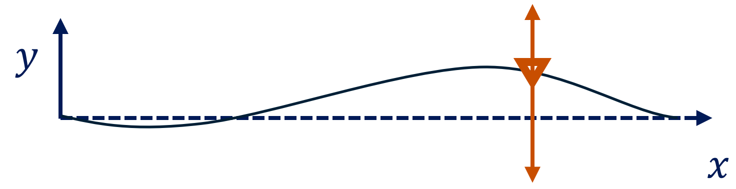

Wind Tunnel Setting

p_c (kPa)	ΔT (K)
68.9	13.3

Duke

Heat Equation (HE) Implementation

$$\underbrace{M_{mn}\ddot{q}_n(t) + C_{mn}\dot{q}_n(t) + G^{(1)}_{mn}q_n(t)}_{\text{Linear plate model}} + \underbrace{D^{(2)}_{mnrp}q_n(t)q_r(t)q_p(t)}_{\text{NL structural stiffness}} + \underbrace{G^{(3)}_{mnr}q_n(t)T_r(t)}_{\text{Thermal coupling}} + \underbrace{Q^{Aero}_m + Q^{static}_m}_{\text{Pressure terms}} = 0$$

$$\underbrace{M^H_{mn}\dot{T}_n(t) + K^H_{mn}T_n(t)}_{\text{Thermal inertia and stiffness}} + \underbrace{Q^0_m + Q^q_{mn}q_n(t) + Q^{\dot{q}}_{mn}\dot{q}_n(t) + Q^{Tq}_{mn}T_n(t)}_{\text{Coupled linear aerodynamic heating}} = 0$$

The HE implementation overpredicts the temperature at and after the shock location for the shock case (chord-wise)

Wind Tunnel Setup

Parameter	Value
M_∞	1.92
p_0	$\approx$ 346 kPa
T_0	$\approx$ 420 K
Δp	0

No shock

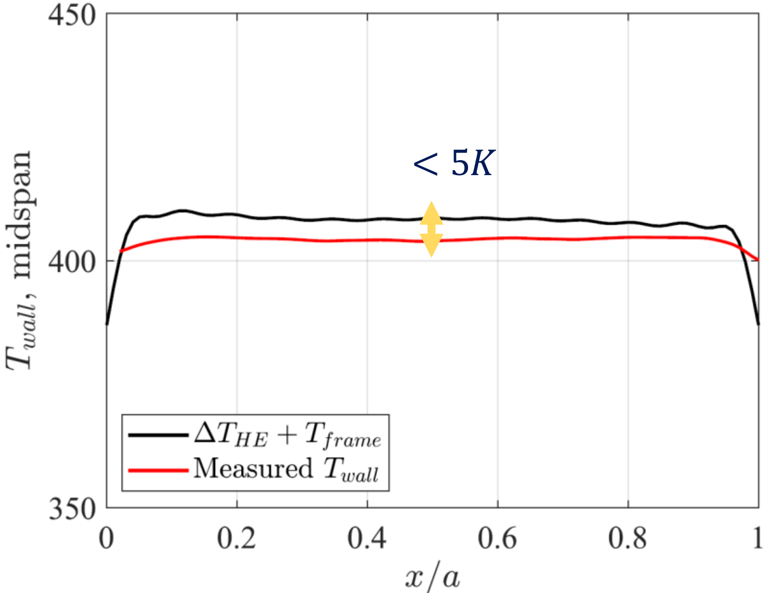

4° Wedge Shock

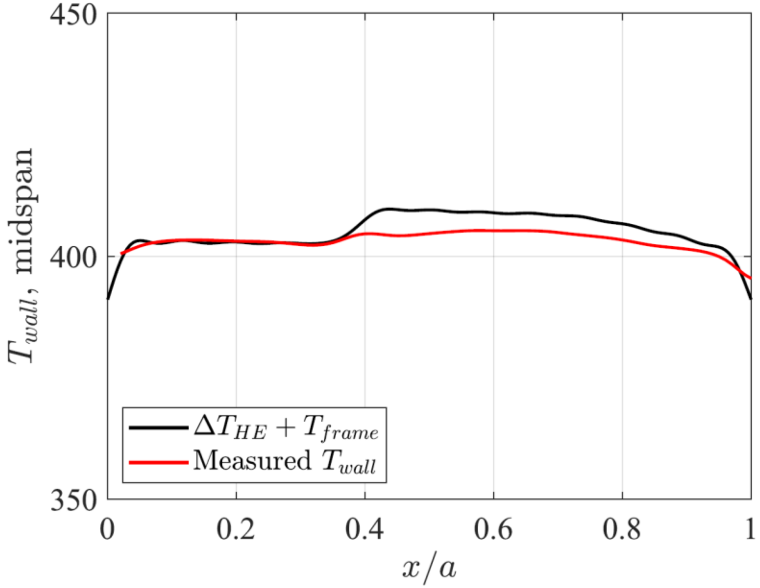

Different setup from the AePW RC-19 case!

$y^+ = 1$

DLTA with a Viscous Shock Impingement

$\theta = 4^\circ$ wedge shock configuration

Mean & SDT deformation
(at ¾ of the panel length)

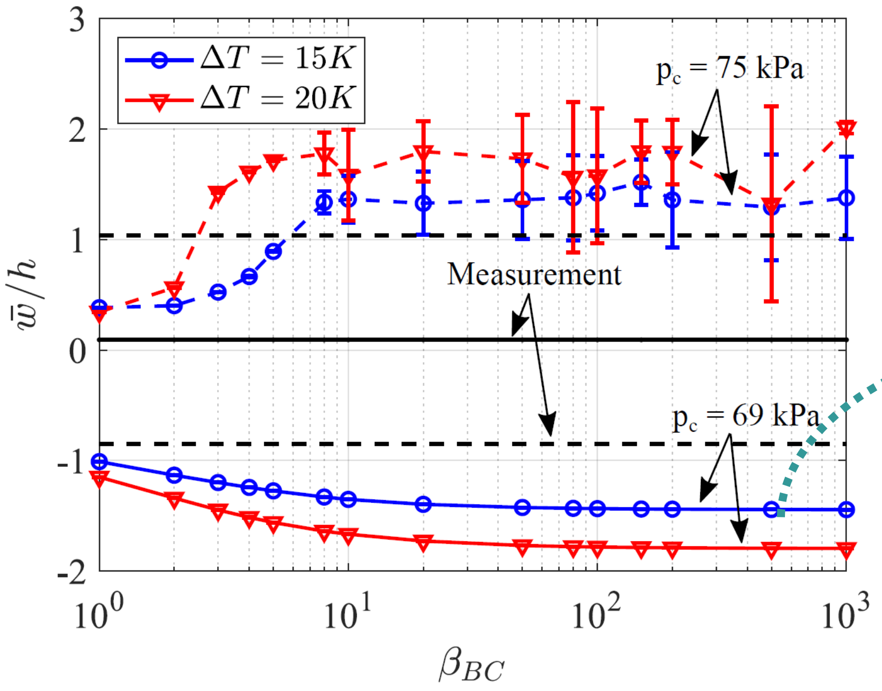

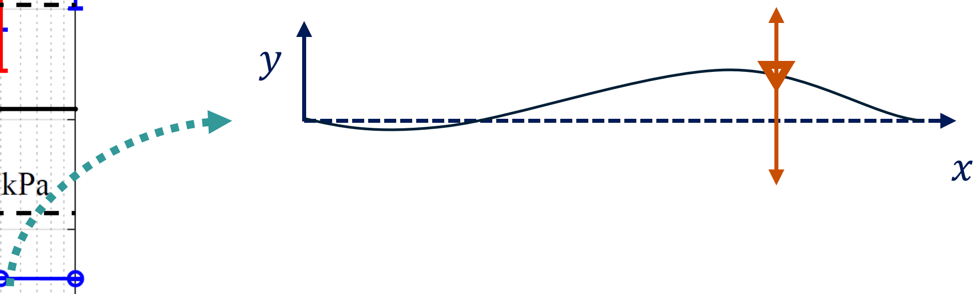

Wind Tunnel Setting

p_c (kPa)	ΔT (K)
68.9	13.3

DLTA with a Viscous Shock Impingement

$\theta = 4^{\circ}$ wedge shock configuration

$y^{+} = 1$

Mean deformation

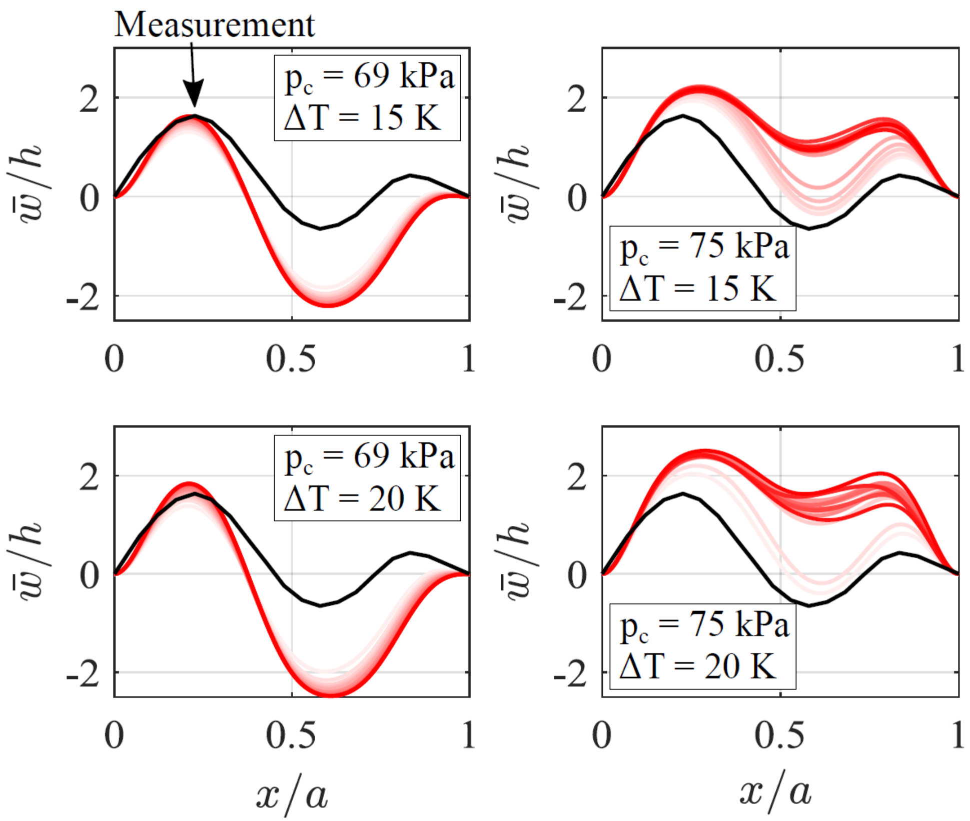

Standard deviation

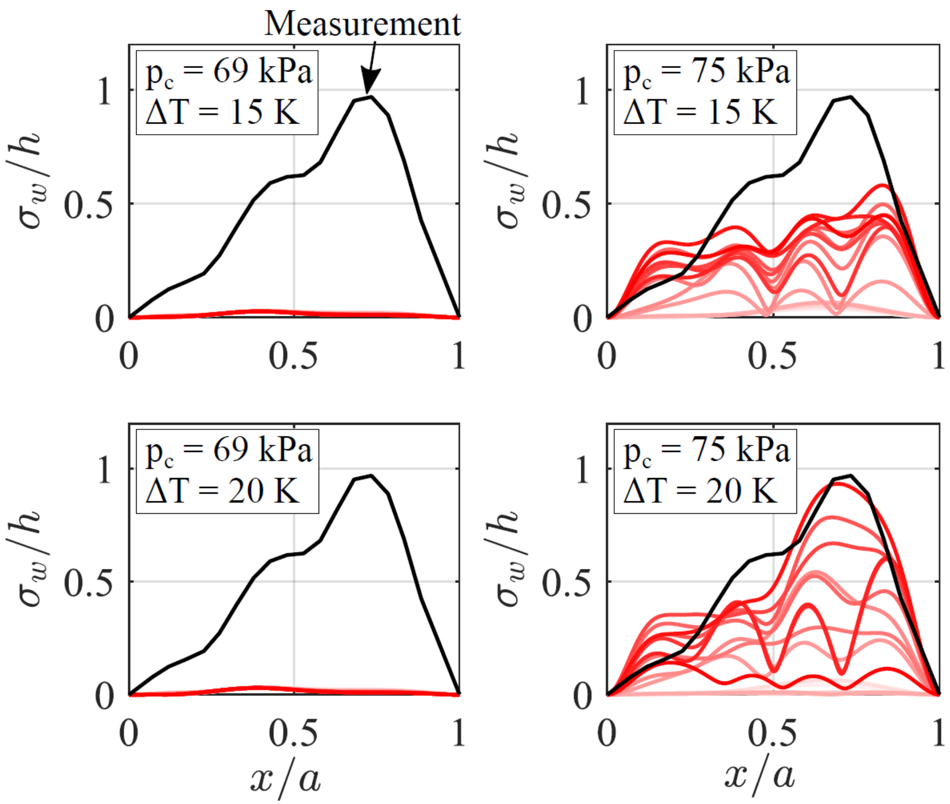

Duke

Future Work

Shock-case configurations

- Investigate the unsteady aerodynamic modeling using DLTA for higher shock wedge angles, particularly for the cases where there is flow separation.

Computational/Experimental Correlation studies

- Expand the RC-19 no-shock configuration using DLTA and CFD data:
    - Most of the issues seen in this study so far with this configuration were linked to the pre-defined flow parameters (Δp and ΔT). Using the CFD solution to obtain these variables can bring further light to the issues seen here.

Duke